International Journal of Earth Sciences (2022) 111:2283–2316
https://doi.org/10.1007/s00531-022-02230-0

ORIGINAL PAPER

Reassessing the polyphase Neoproterozoic evolution of the Punta del Este Terrane, Dom Feliciano Belt, Uruguay

Hernan Silva Lara[1] · S. Siegesmund[1] · S. Oriolo[2] · M. Hueck[1,3] · K. Wemmer[1] · M. A. S. Basei[3] · P. Oyhantçabal[4]

Received: 16 December 2021 / Accepted: 17 July 2022 / Published online: 15 August 2022

Abstract

Some recent models challenge the position and extension of the assumed oceanic basins formed through the break-up of Rodinia, and the tectonic processes involved in the Gondwana assembly, making the investigation of the Early Neoproterozoic record of great relevance. Within the South-American Atlantic margin, the Punta del Este Terrane (PET) of the Dom Feliciano Belt (DFB) comprises a unique Tonian to Ediacaran record, and has a strategic position to reconstruct spatio-temporal relationships with the southern African orogenic belts. Novel zircon U–Pb and Lu–Hf data from the PET basement orthogneisses display Tonian magmatic ages (805–760 Ma) and Hf isotopic signatures indicative of mainly crustal/metasedimentary sources, (Nd T_{DM} ages: 2.2–1.9 Ga, and εHf(t): − 12 to − 4). The basement paragneisses yielded late Paleoproterozoic to Neoproterozoic U–Pb ages, but dominantly positive εHf(t) values. The presented results confirm the correlation of the PET with the Coastal Terrane of the Kaoko Belt, and discard the idea of the Nico Pérez Terrane as a source. Detrital zircon U–Pb and Lu–Hf data from the Rocha Formation yielded a main peak at ca. 660 Ma, with the Neoproterozoic grains showing a εHf(t) between + 1 and + 14. The deposition age of the Rocha Formation is constrained by the youngest detrital zircon age peak (660 Ma), and the beginning of the deposition of the Sierra de Aguirre Formation (580 Ma). The data indicate common sources with the Marmora Terrane, and it is thus proposed that the Rocha Formation belongs to the Gariep Belt, and it was juxtaposed during the Ediacaran to the DFB.

Keywords Kaoko Belt · Gariep Belt · Zircon U–Pb geochronology · Zircon Lu–Hf systematics

Introduction

During the late Neoproterozoic, the interaction of the main cratons that constitutes the present day configuration of South America and Africa, together with several minor crustal blocks, led to the amalgamation of Southwest Gondwana (e.g. Heilbron et al. 2008; Basei et al. 2010; Frimmel et al. 2011; Brito Neves and Fuck 2014; Siegesmund et al. 2018; Konopásek et al. 2020). This process involved several orogenic events and is known as the protracted Pan—African/Brasiliano Orogeny, which extended up to the Cambrian (e.g. Kröner 1984; Rino et al. 2008). From a global perspective, the late Neoproterozoic to Cambrian assembly of Gondwana was the result of the convergence that followed the early Neoproterozoic Rodinia break-up (e.g. Oriolo et al. 2017). However, the participation of many southern South American and African crustal blocks in Rodinia has been challenged and, therefore, the early Neoproterozoic geologic record of these regions may not necessarily record Rodinia break-up (e.g. Cordani et al. 2003; Kröner and Cordani 2003; Oriolo et al. 2017). In this context, Tonian units in Western Gondwana are the key to understanding the transition from the break-up of Rodinia to the assembly of Gondwana.

The Punta del Este Terrane in the southern Brasiliano Dom Feliciano Belt, hosts the record of Tonian tectonomagmatic processes, which have alternatively been interpreted as the result of subduction or continental rifting (e.g. Lenz

✉ Hernan Silva Lara
hsilva@fcien.edu.uy

[1] Department of Structural Geology and Geodynamics, Geoscience Centre, University of Göttingen, Goldschmidtstr. 3, 37077 Göttingen, Germany

[2] CONICET-Universidad de Buenos Aires, Instituto de Geociencias Básicas, Aplicadas y Ambientales de Buenos Aires (IGEBA), Buenos Aires, Argentina

[3] Geosciences Institute, University of São Paulo, São Paulo, Brazil

[4] Instituto de Ciencias Geológicas, Universidad de la República, Montevideo, Uruguay

et al. 2011, 2012; Masquelin et al. 2012; Martil et al. 2017; Konopasek et al. 2017, 2020; Will et al. 2019; De Toni et al. 2021). In addition, this South American Terrane, located close to the African Gariep Belt before the opening of the Atlantic Ocean, is a fundamental piece for reconstructing the spatio-temporal relationships between these orogenic belts. Magmatic (805–760 Ma) and metamorphic ages (660–640 Ma) of the basement of the Punta del Este Terrane, resemble those of the Coastal Terrane of the Kaoko Belt. Both terranes have been previously correlated (e.g. Oyhantcabal et al. 2009; Kónopasek et al. 2017; Will et al. 2019). However, the tectonic setting of the Tonian magmatism has been discussed considerably, mostly based on different interpretations of its geochemical and isotopic signatures. On the other hand, the Punta del Este Terrane has the only metasedimentary successions on the eastern side of the Granite Belt of the Dom Feliciano Belt, among which the Rocha Formation is the most significant (Figs. 1, 2). This low-grade metasedimentary formation has been envisaged as a turbidite sequence, that may be correlated with the Oranjemund Group of the African Gariep Belt (Basei et al. 2005; Abre et al. 2020), but the nature of the basin to which it is associated, its isotopic signature, sources and depositional age are still under discussion.

In this study, we present novel zircon U–Pb and Lu–Hf data of ortho- and paragneisses of the Punta del Este Terrane basement and the overlying Rocha Formation, combined with geological and structural data. The results are evaluated to determine the timing and isotopic signatures of the main tectonomagmatic, sedimentary and metamorphic events in the Punta del Este Terrane and provide a comprehensive revised tectonic evolution from the Tonian to the Ediacaran.

Geological framework

On both sides of the South Atlantic Ocean, a series of orogenic systems record the amalgamation of Gondwana in the late Neoproterozoic during the Pan African/Brasiliano orogenic cycle (e.g. Heilbron et al. 2008; Basei et al. 2010; Frimmel et al. 2011; Brito Neves and Fuck 2014; Siegesmund et al. 2018; Konopasek et al. 2020; Caxito et al. 2021, 2022). In its southern portion, this system resulted from the interaction between the South American Rio de La Plata craton and the African Kalahari and Congo cratons, together with several minor continental fragments (Fig. 1). This process resulted in the formation of the Dom Feliciano Belt in South America, and the Kaoko, Damara and Gariep belts on the African side (Fig. 1, Frimmel et al. 2002, 2011; Passchier et al. 2002, 2016; Goscombe et al. 2005, 2017a, b, 2018; Konopasek et al. 2005, 2008, 2016; Goscombe and Gray 2008; Frimmel 2018).

The Dom Feliciano Belt (Fig. 2) extends along the South American eastern margin for over 1400 km, from the Florianópolis region in southern Brazil to southernmost Uruguay (e.g. Basei et al. 2000; Philipp et al. 2016; Hueck et al. 2018). Recent studies also show that this belt probably continues southwards in the Argentinian continental shelf, constituting the basement of the Ventania Belt (Rapela et al. 2011; Ballivian Justiniano et al. 2020; Christiansen et al. 2021). It is divided into an Eastern and a Western sector, separated by the Sierra Ballena–Major Gercino transcurrent system (e.g. Oriolo et al. 2016; Masquelin et al. 2017; Oyhantçabal et al. 2018; Hueck et al. 2019). This lineament marks the border between terranes with a series of differences in the geologic signatures, particularly in the ages of the basement, and the geochemistry and isotopic signatures of the Ediacaran magmatism (Lara et al. 2020). As with most of the orogenic belts along the Atlantic margins of South America and Africa, the evolution of the Dom Feliciano Belt has traditionally been interpreted in terms of subduction of oceanic crust and subsequent collision (Basei et al. 2000, 2005, 2008, 2018; Bitencourt and Nardi 2000; Goscombe and Gray 2008; Konopasek et al. 2008; Oyhantçabal et al. 2009; Saalmann et al. 2011; Frimmel et al. 2011; Oriolo et al. 2016; Passchier et al. 2016; Philipp et al. 2016; Goscombe et al. 2017a; Arena et al. 2016; Frimmel 2018; Hueck et al. 2019; Ramos et al. 2018, 2020; Will et al. 2019, 2020). More recently, however, tectonic models arguing intracontinental processes for the region, challenge the extent and location of the assumed oceanic basins between the different crustal blocks (Konopasek et al. 2017, 2020; Percival et al. 2021).

Several minor continental fragments involved in this large orogenic process are preserved as basement inliers, characterized by Archean to Paleoproterozoic ages (Figs. 1, 2, Hueck et al. 2022). Among them, the Nico Pérez Terrane is of particular interest for the evolution of the region. This Archean to Paleoproterozoic block (e.g. Hartmann et al. 2001; Santos et al. 2003; Gaucher et al. 2011, 2014; Oyhantçabal et al. 2012; Oriolo et al. 2016; Masquelin et al. 2021) records several deformation and metamorphic processes related to the amalgamation of southwest Gondwana (e.g. Oriolo et al. 2016; Masquelin et al. 2017; Oyhantçabal et al. 2018), being interpreted as a marginal piece of the Congo Craton during the Neoproterozoic (e.g. Oyhantçabal et al. 2011, 2018; Rapela et al. 2011; Oriolo et al. 2016; Percival et al. 2021; Hueck et al. 2022).

In contrast to these older basement fragments two Tonian–Cryogenian blocks are recognized within the Dom Feliciano Belt. They are the São Gabriel and Punta del Este Terrane, located, respectively, in the western and eastern sectors of the belt (Fig. 2). Both blocks comprise partially overlapping magmatic ages, but have contrasting isotopic signatures in which the first one is predominantly juvenile,

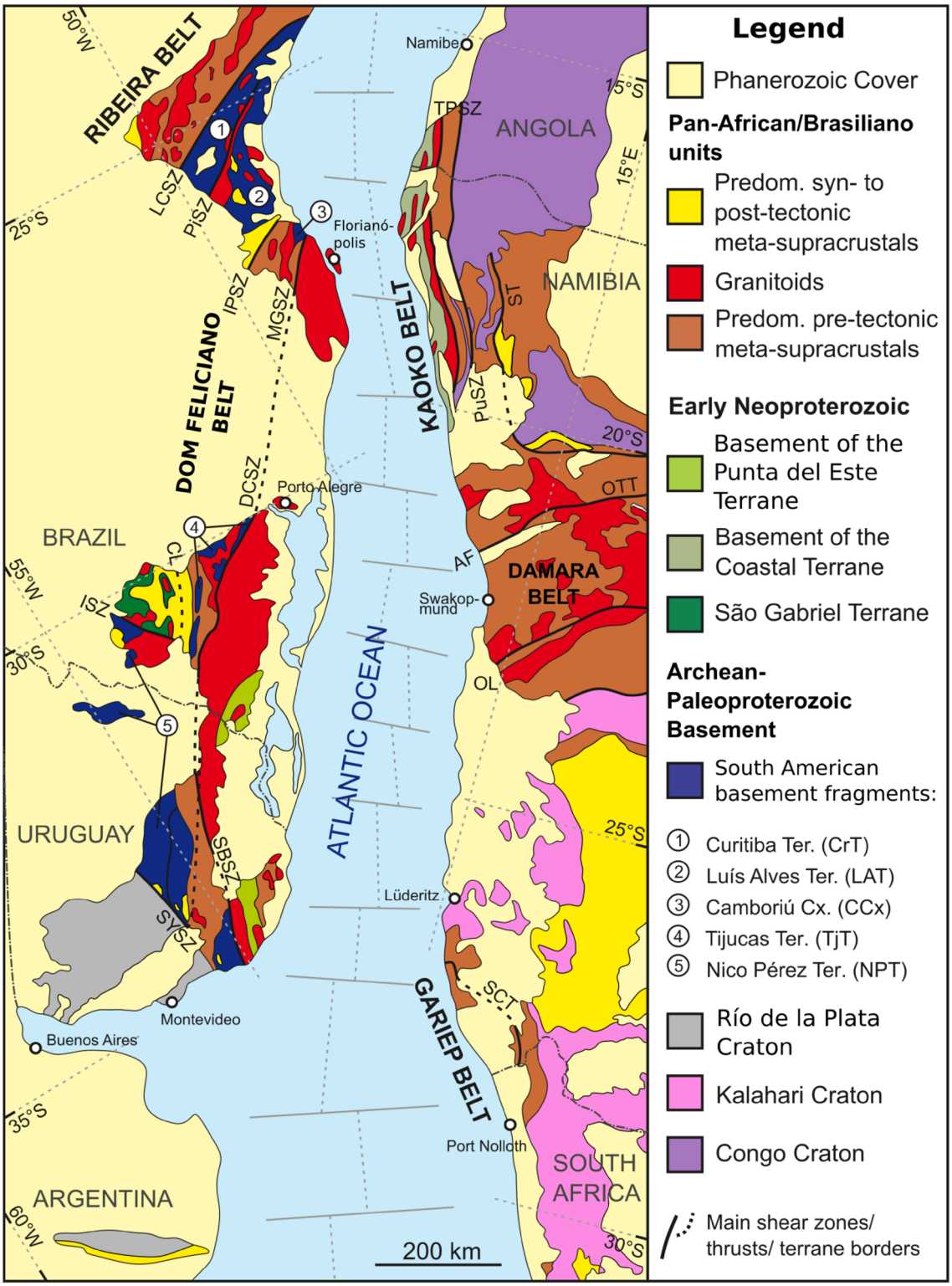

Fig. 1 Simplified geological map of the Atlantic coastal regions of southern South America and Africa with relative positions reconstructed before the opening of the Atlantic Ocean. Main shear zones (SZs): SYSZ: Sarandí del Yí; SBSZ: Sierra Ballena; SSSZ: Sierra de Sosa; ISZ: Ibaré; CL: Caçapava Lineament; DCSZ: Dorsal do Canguçu; MGSZ: Major Gercino; IPSZ: Itajaí-Perimbó; PiSZ: Piˆen; LCSZ: Lancinha-Cubatão; TPSZ: Three Palms; PuSZ: Purros; ST: Sesfontein Thrust; AF: Autseib Fault; OTT: Otjohorongo Thrust; OL: Okahandja Lineament; SCT: Schakalsberge Thrust (modified after Hueck et al. 2022)

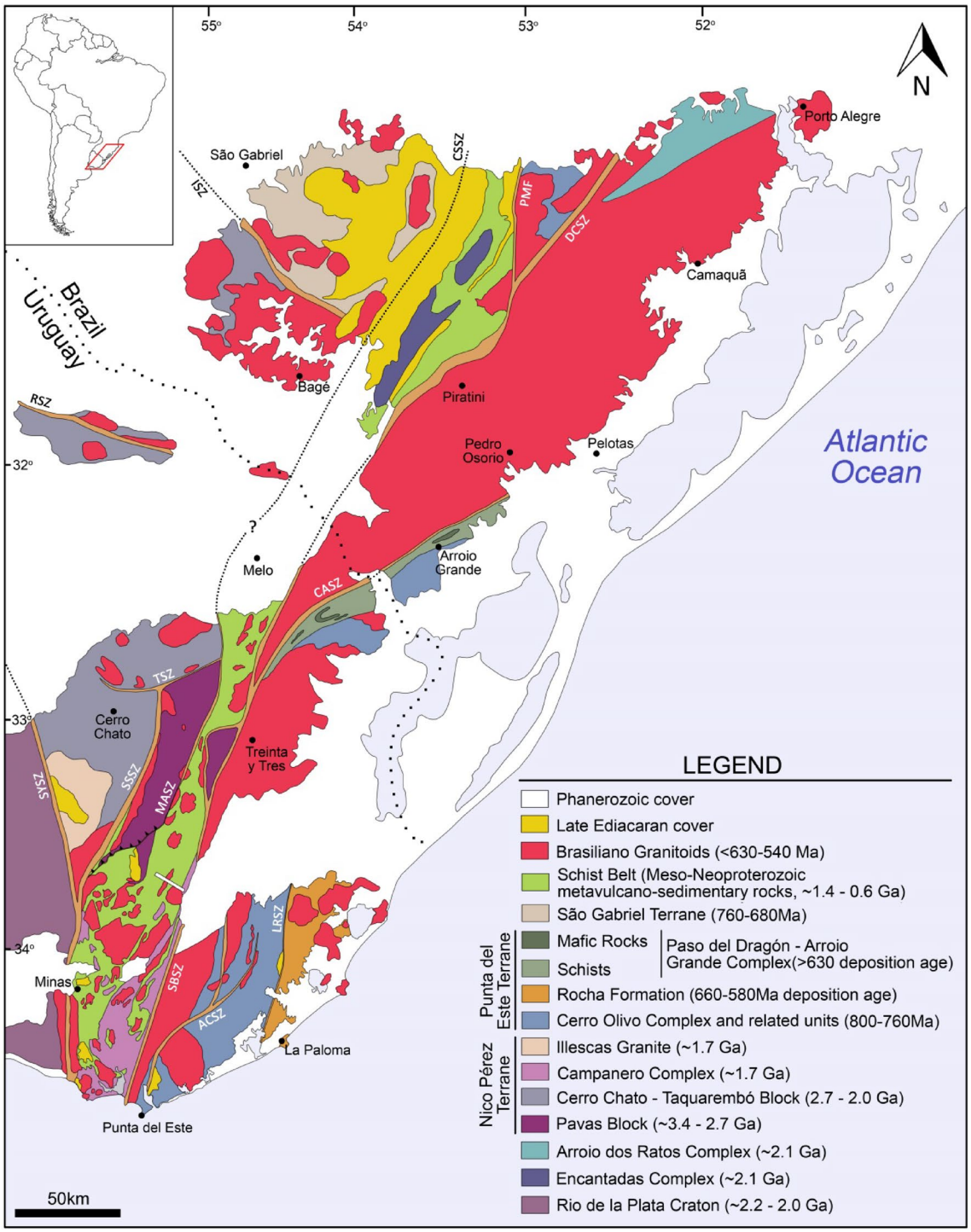

Fig. 2 Geological sketch of the Dom Feliciano Belt. SBSZ: Sierra Ballena Shear Zone, ACSZ: Alférez Cordillera Shear Zone, LRSZ: Laguna de Rocha Shear Zone, SYSZ: Sarandí del Yí Shear Zone, MASZ: María Albina Shear Zone, SSSZ: Sierra de Zosa Shear Zone, CASZ: Cerros de Amaro Shear Zone, RSZ: Rivera Shear Zone, ISZ: Ibaré Shear Zone, DCSZ: Dorsal do Canguçu Shear Zone, PMSZ: Paso do Marinheiro Shear Zone, CSSZ: Caçapava do Sul Shear Zone [modified after Masquelin el al. (2017) and Hueck et al. 2018, 2020a, b)]

whereas the second clearly involved the reworking of crustal sources. The São Gabriel Terrane comprises two main magmatic associations, interpreted as two different magmatic arcs, together with passive margin associations and relict ophiolite complexes (Philipp et al. 2018, 2021). The first magmatic association presents ages ranging from 890 to

860 Ma and is interpreted as an intraoceanic arc (Pasinho Arc, e.g. Phillip et al. 2018 and references therein). The second one represents a juvenile Cordilleran arc, with ages ranging from 770 to 720 Ma (São Gabriel Arc). This last arc magmatism is followed by post-collisional intrusions ranging from 700 to 680 Ma (Phillip et al. 2018).

The Punta del Este Terrane

This terrane represents the main expression of Tonian rocks in the eastern domain of the Dom Feliciano Belt (Figs. 2, 3). Since its original definition (Preciozzi et al. 1999), the boundaries, extension and units that comprise this block have been subject of considerable discussion. The modern definition of the terrane includes all units to the east of the Sierra Ballena Shear Zone (Bosi and Gaucher 2004; Oyhantçabal et al., 2010; Gaucher et al. 2014; Will et al. 2019). These are comprised of (a) a high-grade basement represented by the Cerro Olivo Complex and minor chronocorrelate gneissic inliers and xenolithes along the extension of the Dom Feliciano Belt, such as the Piratini and the Chacará das Pedras gneisses, and the Varzéa do Capivarita and Porto Belo Complexes (Fig. 1, Gross et al. 2006; Koester et al. 2016; Philipp et al. 2016; Martil 2016; Martil et al. 2011, 2017; Cruz et al. 2017; Tambara et al. 2019; De Toni et al. 2020); (b) the low-grade metasedimentary Rocha

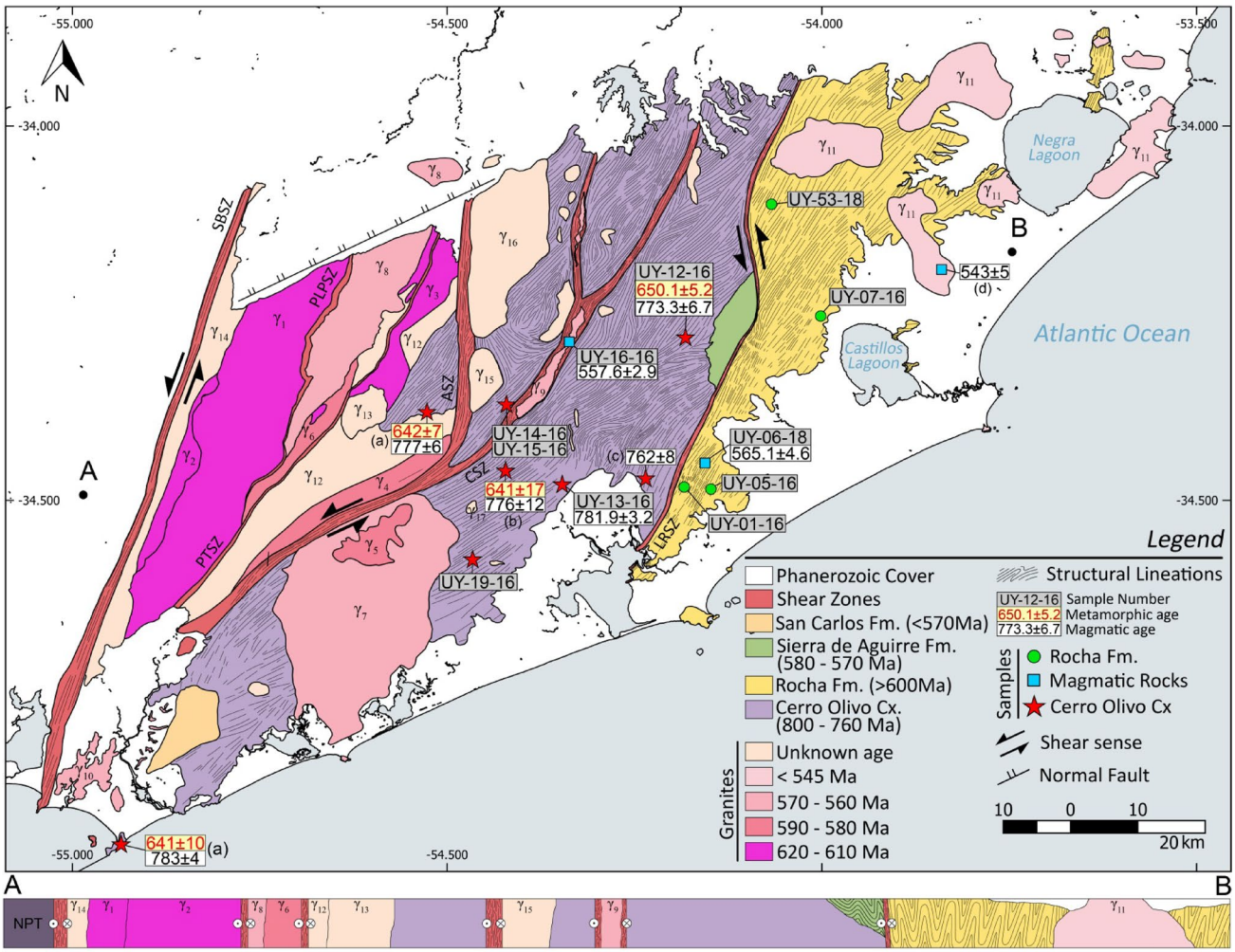

Fig. 3 Geological map and profile of the main exposures of the Punta del Este Terrane based on Spoturno et al. (2012) and Silva Lara et al. (2021). **a** Age data from Will et al. (2019), **b** after Oyhantçabal et al. (2009), **c** after Hartmann et al. (2002), **d** Basei et al. (2013). SBSZ: Sierra Ballena Shear Zone, PLPSZ: Puntas de las Palmas Shear Zone, PTSZ: Paso de los Talas Shear Zone, ASZ: Álferez Shear Zone, CSZ: Cordillera Shear Zone, LRSZ: Laguna de Rocha Shear Zone. Granites: γ1—Aiguá granite, γ2—Aiguá mylonitic granite, γ3—Valdivia granite, γ4—Puntas del Arroyo Manantiales mylonitic granite, γ5—Sierra de Garzón granite, γ6—Cerro Catedral Unit, γ7—José Ignacio Granite, γ8—Florencia granite, γ9—Rocha Granite, γ10—Maldonado granite, γ11—Santa Teresa Granitic Complex, γ12—Cerro Áspero Granite, γ13—Puntas del Arroyo Rocha granite, γ14—Sierra de los Caracoles mylonitic granite, γ15—El Pintor granite, γ16—Velázquez granite

Formation, the main cover succession of the terrane; (c) the metavolcano-sedimentary Paso del Dragón—Arroio Grande Complex; (d) voluminous Ediacaran granitic magmatism, mostly grouped within the Aiguá Batholith; (e) minor Ediacaran volcanic deposits and basins, the most significant of which is the Sierra de Aguirre Formation; and (f) relics of late-orogenic volcano-sedimentary deposits, represented by the San Carlos Formation.

The Basement

The Cerro Olivo Complex (Fig. 3) is a high-grade metamorphic complex, consisting of orthoderived and paraderived units (Masquelin et al. 2005, 2010). The complex shows a poliphasic evolution: The main magmatic ages of the orthogneisic rocks range from 800 to 760 Ma, with inherited zircon grains yielding Paleo- to Mesoproterozoic ages (e.g. Oyhantçabal et al. 2009; Lenz et al. 2011; Masquelin et al. 2012). Other minor orthogneissicse units comprised within this block, the Arroio Pedrado, Sarandí de Barceló and Mendizábal gneisses have magmatic ages between 680 and 665 Ma, though their tectonic significance is still unclear (Phillip and Machado 2002; Gaucher et al. 2014; Vieira et al. 2016, 2019; Will et al. 2019).

Granulite-facies metamorphism and subsequent migmatization affected the basement from ca. 660 to 640 Ma (Preciozzi et al. 1999; Gross et al. 2009; Oyhantçabal et al. 2009; Basei et al. 2011; Lenz et al. 2011; Masquelin et al. 2012; Peel et al. 2018; Will et al. 2019; Vieira et al. 2019). This event is coeval with minor mafic sin- to post-deformational magmatism, with ages ranging from 659 to 635 Ma (Lenz et al. 2014).

The stratigraphy of the complex is still controversial, and the relationship between the ortho- and paragneisses is complex. A compilation of the different stratigraphic proposals for the Cerro Olivo Complex is presented by Masquelin et al. (2005), summarizing the results of Masquelin (1990, 2001), Masquelin et al. (2002) and Preciozzi et al. (1993, 1999, 2002). Most of the models propose that the mafic and paraderived rocks are the oldest of the complex, based on limited structural field observations (Masquelin et al. 2001, 2005, 2006).

The Rocha Formation

The Rocha Formation (Betucci and Burgueño 1993) is the main low-grade supracrustal succession of the Punta del Este Terrane. It is a metasedimentary sequence built up of metapelites and metasandstones which underwent greenschist facies metamorphism (Betucci and Burgueño 1993; Menezes 2010). This unit is in tectonic contact with the Cerro Olivo Complex and the Sierra de Aguirre Formation through the sinistral Laguna de Rocha Shear Zone (Masquelin 2005; Silva Lara et al. 2021).

Based on locally preserved sedimentary structures, Basei et al. (2005) proposed a transitional fluvial to tidal plain environment for the deposition of the Rocha Formation. More recently, and based on lithological and geochemical similarities, this unit was interpreted as a turbidite sequence linked to a magmatic arc (Blanco et al. 2014; Abre et al. 2020). Tectonic reconstructions have correlated the Rocha Formation with the Oranjemund Group of the Gariep Belt (Basei et al. 2005; Gaucher et al. 2009; Abre et al. 2020). Constraints on the timing of deposition were first estimated at > 600 Ma based on the youngest recognized cluster of detrital zircon (Basei et al. 2005), whereas more recent contributions have proposed a maximum deposition age of 569 ± 10 Ma (Abre et al. 2020), determined by the youngest detrital zircon.

Though little studied, two contrasting models for the structural style of the unit have been proposed. Masquelin and Tabó (1990) proposed a structural evolution of four main deformation phases: D_1 represents the transposition of S_0 by the cleavage S_1, D_2 that developed isoclinal folds with sub-vertical axes plunging to N210°–230°; D_3 with open folds of sub-vertical axial planes with a N130° trend; and D_4 with chevron folds. On the other hand, Menezes (2010) proposed three main deformation phases: D_1 characterized by open to tight folds with sub-horizontal axes and axial planes with high-angle dips to the NW and SE, and associated S_1 cleavage development; D_2, characterized by open folds with sub-vertical fold axes, affecting the S_1; and D_3, characterized by crenulation cleavage with sub-horizontal axial planes and axes.

The Laguna de Rocha Shear Zone

This shear zone is the tectonic limit between the Cerro Olivo Complex and the Rocha Formation. The Sierra de Aguirre Formation, which overlies the Cerro Olivo Complex, is also in tectonic contact with the Rocha Formation through this shear zone. The shear zone was first described as a cataclastic zone between the Rocha and the Sierra de Aguirre Formation (Masquelin and Tabó 1990). Similarly, Bossi and Navarro (1991) and Campal and Gancio (1993) suggest that the tectonic limit between these two supracrustal units is defined by a sub-vertical brittle fault. Campal and Shipilov (2005) propose that the limit between these two formations is delineated by a mylonitic to cataclastic zone. Masquelin (2005) defines this tectonic contact as a shear zone named the Laguna de Rocha Shear Zone, and extended its significance to the region, proposing that the structure also represents the limit between the Cerro Olivo Complex and the Rocha Formation. More recently, Silva Lara et al.

(2021) described the kinematics and time of deformation of the shear zone, based on field features, quartz CPO analysis and K–Ar ages. The structure is a sinistral transcurrent shear zone, with deformation conditions within the greenschist facies. K–Ar ages in syn-kinematic muscovites of the shear zone yielded an age of 564 ± 6.1 Ma, interpreted as syn-kinematic crystallization ages. Clay-sized white mica fractions yielding ages between 535 and 525 Ma, are interpreted as representative of the end of the ductile deformation within the shear zone. These results are similar to the ones reported for the neighboring shear zones (e.g. Hueck et al. 2017, 2020a, b).

The Paso del Dragón–Arroio Grande Complex

The Paso del Dragón–Arroio Grande Complex is another cover succession of the Punta del Este Terrane, classically correlated with the Rocha Formation (e.g. Peel et al. 2018). It comprises two tectonically intercalated units, a metavolcano-sedimentary succession, composed of mica-schists, quartzites and minor metavolcanic rocks, and a metamafic–ultramafic association, with subordinated marbles (Peel et al. 2018; Chaves Ramos et al. 2018). The depositional age of the metasediments of the complex remains controversial. The youngest detrital zircon peak reached a Cryogenian age (660–650 Ma, Gaucher et al. 2014; Beloni et al. 2016; Peel et al. 2018; Chaves Ramos et al. 2018), while zircon crystals younger than 650 Ma are interpreted as associated with metasomatic reactions related to the magmatic activity and the activity of the shear zones (Chaves Ramos et al. 2018). Different ages for the deposition and metamorphism of this unit have been suggested based on the results of both, metasedimentary and metamafic units (Klein et al. 2018; Chaves Ramos et al. 2018; Peel et al. 2018; Will et al. 2019).

The Ediacaran granitic magmatism

Felsic volcanic-intrusive magmatism constitutes an important part of the Ediacaran history of the Punta del Este Terrane, recording a protracted evolution (ca. 630–543 Ma) and frequent links with the large-scale shear zones of the Dom Feliciano Belt. Associated with this granitic magmatism, several minor volcanic units can be found. The main occurrence is the Sierra de Aguirre Formation (Masquelin and Tabó 1990), which mainly comprises volcaniclastic rocks intercalated with minor lava flows (Campal and Schipilov 2005; Silva Lara et al. 2021; Will et al. 2021). These were deposited between ca. 580 and 570 Ma (Hartmann et al. 2002; Silva Lara et al. 2021; Will et al. 2021) in a restricted basin bounded by the Laguna de Rocha Shear Zone (Silva Lara et al. 2021). This formation is interpreted to have been deposited in an extensional or transtensional setting, later inverted by a single-phase folding coeval to the transpressional activity of the Laguna de Rocha Shear Zone (Masquelin 2005; Silva Lara et al. 2021).

Analytical techniques

U–Pb geochronology

An extensive geochronological investigation was carried out to achieve a comprehensive evolution model of the Punta del Este Terrane and, in particular, constrain the deposition and deformation age of the Rocha Formation, one of the major outstanding questions in the region. For that, geochronological analyses were carried out in the basement of the sequence, in the meta sedimentary rocks themselves, and in key intrusive bodies with clear links to the structural evolution of the sequence.

SHRIMP and LA-ICP-MS U–Pb zircon analyses were carried out at the Geochronological Research Center of the Geosciences Institute in the São Paulo University (CPGeo—USP). A total of three SHRIMP analyses and eight LA-ICP-MS analyses were carried out. SHRIMP age determinations were performed in orthogneiss samples from the Cerro Olivo Complex as well as in samples from a rhyolithic dyke intrusive in the Rocha Formation and from the Rocha Granite, whereas the rest of the presented geochronological data correspond to LA-ICP-MS analyses. Analytical procedures are provided in Appendix A and the analytical data in Appendix B, together with the interpretation of each spot analysis. Concordia ages were calculated using Isoplot/Ex 4.15 (Ludwig 2008). For most of the samples, grains which produced > 10% discordant results were not taken into account for the age calculations.

The age spectra of detrital zircon of the analyzed samples in this work are presented as kernel density plots (KDP) and histograms plotted using DensityPlotter (Vermeesch 2012). To avoid acquiring ages younger than the true maximum depositional age due to laboratory or field contamination, as well as lead loss (Coutts et al. 2019; Andersen et al. 2019), we used the youngest peak age calculated considering age probability contributions from at least three analyses, calculated with the AgePick spreadsheet of the University of Arizona LaserChron Center (www.geo.arizona.edu/alc).

Lu–Hf isotopes

Lu–Hf isotopic measurements were carried out at the Geochronological Research Center of the Geosciences Institute of the São Paulo University (CPGeo—USP) using a LA-ICP-MS. Further analytical procedures and results are given in Appendix C. Spot analyses were performed as

close as possible to the previous concordant U–Pb spots in the same crystals, and εHf and T_{DM} parameters were calculated after Yang et al. (2007) using the $^{206}Pb/^{238}U$ ages obtained from the corresponding U–Pb spot analyses.

Sm–Nd analysis

Sm–Nd analyses were carried out in three samples from the Rocha Formation at the Geochemistry and Isotope Geology Department of the Georg-August Universität Göttingen, using a thermal ionisation mass spectrometer (TIMS—Finnigan MAT 262) equipped with nine movable faraday collectors that can be paired with nine 1011 and one 1012 Ω amplifiers.

Lithology and structure of the studied units

Cerro Olivo Complex

The main exposures of the Cerro Olivo Complex crop out as an elongated body about 140 km long and 40 km wide at the southeastern portion of the Dom Feliciano Belt (Fig. 3). It is composed of ortho- and paraderived gneisses, which mostly show a metamorphic grade between granulite and upper amphibolite facies. The structural grain presents a general NNE trend, but large deviations from the general trend can be observed locally.

The main lithologies recognized and sampled in this work are: (a) banded felsic orthogneisses, composed of quartz, plagioclase and perthitic feldspar, with variable amounts of biotite and orthopyroxene, protomylonitic overprint; (b) mafic granulites, composed mostly of orthopyroxene, quartz and plagioclase, with hornblende, Ti–rich biotite and clinopyroxene as main accessories, characterized by a granoblastic texture; (c) pelitic gneisses, composed of quartz, plagioclase, microcline, orthoclase, garnet, biotite, and sillimanite, with accessory muscovite, opaque minerals, zircon, apatite, epidote and pyroxene, characterized by a diffuse and sometimes protomylonitic banding; (d) calc-silicate rocks, composed of calcite, wollastonite, quartz, clinopyroxene and garnet. Other lithologies are also present in this unit, such as quartzites, muscovite-biotite gneisses and different kinds of migmatites.

Rocha Formation

Lithological characterization

Outcrops of the formation are scarce and not continuous, with the best exposures being observed at the Uruguayan Atlantic shore. Metapelites are the dominant lithology of the unit, with significant occurrences of metasandstones and metawackes only in the coastal region.

At outcrop scale the metasandstones and metawackes show a general quartzitic composition, with variable amount of detrital muscovite. In the northern portion of the unit, a conspicuous carbonatic component is recognized within the matrix. Petrographically, they are poorly sorted, very fine- to fine-grained rocks with up to 30% of matrix (Fig. 4a, b). They are composed of subangular to subrounded clasts of quartz (70–85%), feldspar (10–20%) and lithics (< 5%). The quartz clasts are either monocrystalline or polycrystalline, showing different internal microstructures, such as undulose extinction, subgrains, and evidence of dynamic recrystallization by means of bulging and sub-grain rotation. The feldspar clasts are albitized plagioclase and K-feldspar. Some grains are also partly or completely replaced by sericite. The lithic clasts are mostly muscovite-quartz-schist fragments. Detrital biotite, totally or partially transformed to chlorite, as well as detrital and neoformed muscovite, were also recognized. The matrix is composed of fine-grained quartz, muscovite and minor feldspar. Epidote, titanite, apatite, tourmaline, zircon, rutile, calcite and magnetite are the main accessory minerals.

The metapelites show a composition dominated by fine-grained quartz, minor feldspar and variable amounts of fine-grained white mica. This last feature, together with variations in the grain size, determines a primary lamination in the metapelites (Fig. 4c–f).

Structure

In spite of its deformation, some primary structures are still preserved, such as heterolithic structures, lamination, cross lamination and erosive surfaces (Fig. 5a–f). However, these structures are scarce and the whole sequence is strongly deformed, thus preventing the reconstruction of a full stratigraphic column. The Rocha Formation is characterized by two different fold geometries described in this work as F_1 and F_2. F_1 folds are isoclinal and affect the bedding S_0 (Fig. 6a, b). The cleavage (S_1) associated with these folds could not be recognized and is supposed to be transposed by the S_2 (Fig. 6c). The measured F_1 folds show fold axes plunging 70–90° to the 210°. F_2 folds re-fold the S_0 and show tight geometry, with an associated axial plane cleavage S_2. This cleavage constitutes the main reference surface of the formation in most parts of the outcrops, where it is slightly oblique or nearly parallel to the S_0. F_2 folds show axes plunging 5°–20° to the SSW, and axial planes with a general 030° trend, nearly vertical or dipping slightly to the NW or SE. F_2 folds get

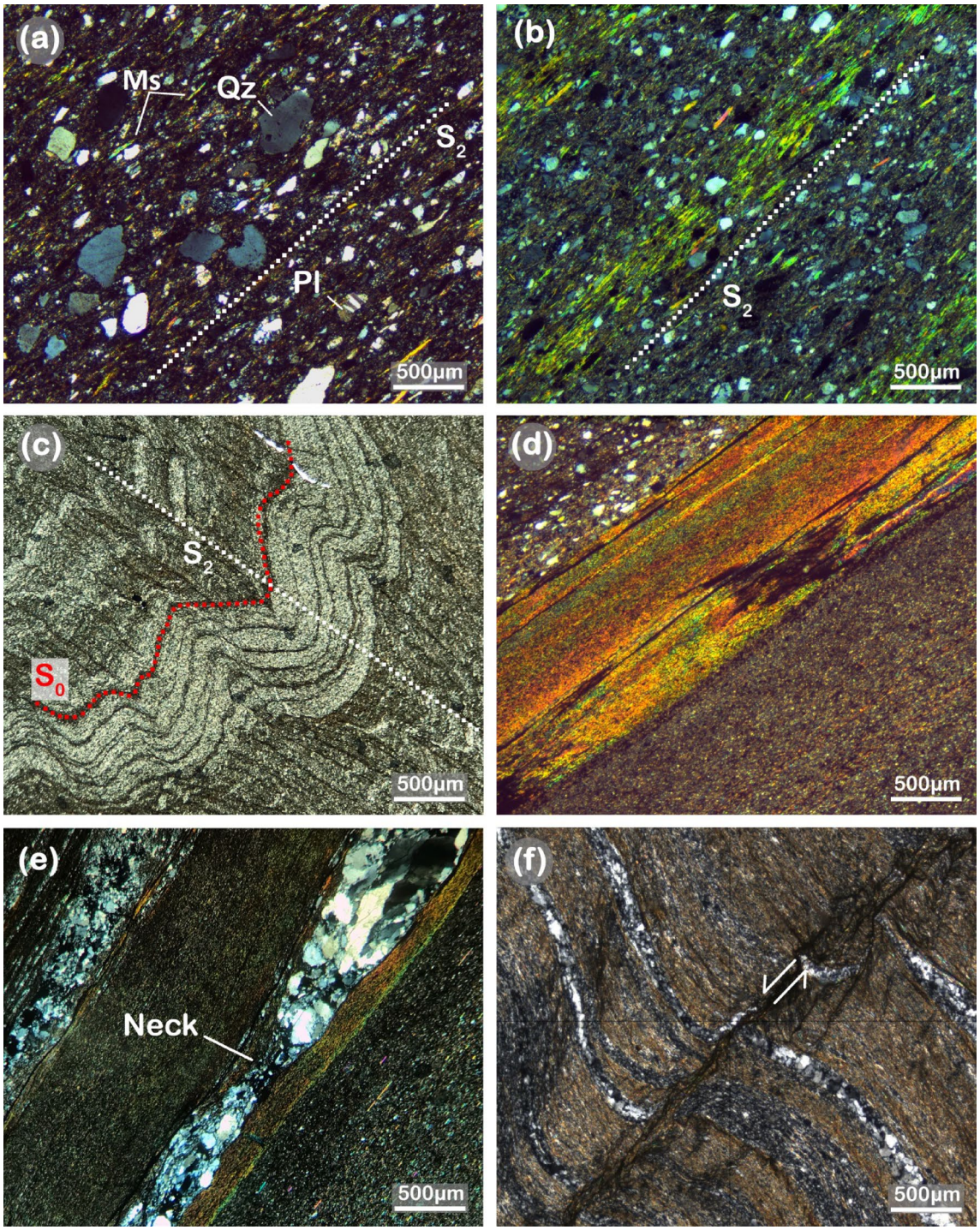

Fig. 4 Petrographic and microstructural aspects of the Rocha Formation: **a** fine-grained, poorly sorted quartz-feldspathic metasandstone, showing a cleavage made up of muscovite; **b** fine-grained quartz-feldspathic metasandstone showing compositional layering determined by the variation in the muscovite content; **c** intersection of the bedding and the cleavage in the hinge of a folded metapelite; **d** layers of different grain size and composition; **e** Quartz veins parallel to the cleavage showing boudinage in a metapelite; **f** laminated metapelite with brittle structures

progressively tighter from E to W, and in the proximity of the Laguna de Rocha Shear Zone they acquire a near isoclinal geometry (Fig. 7).

Quartz veins related to pressure-solution processes are conspicuous and at least two generations can be observed. The older one is strongly deformed and shows boudinage

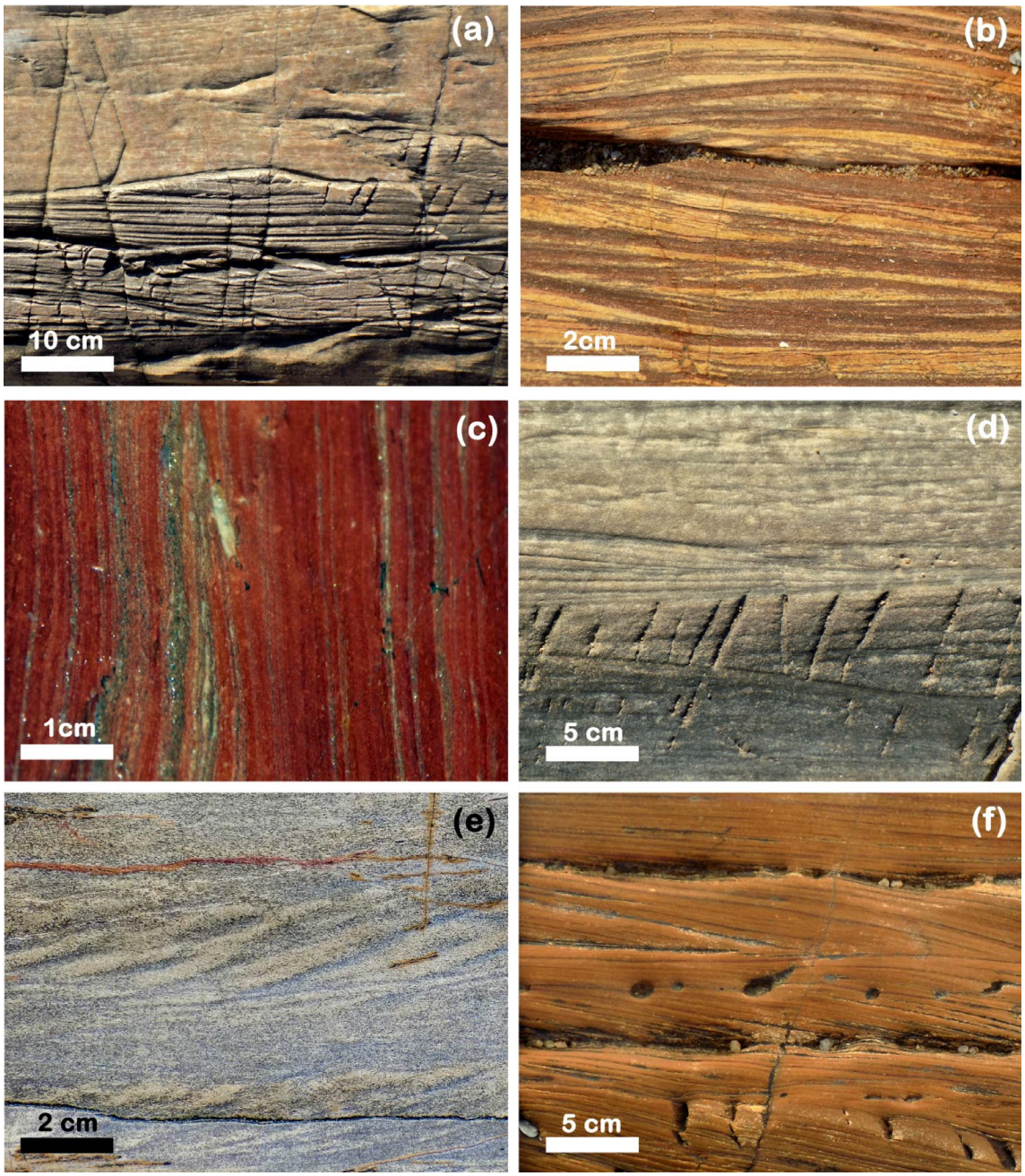

Fig. 5 Sedimentary features of the Rocha Formation: **a** Erosive surfaces between sand beds; **b** heterolithic structures: lenses and intercalation between silt and clay fractions; **c** lamination defined by alternating layers of silt and fine-grained sand; **d** terminations of cross bedding sets; **e** metasandstone layer with diagonal lamination; **f** beds of sandstone with cross laminations

structures parallel to the S_2 (Fig. 4e), while the younger one cross-cuts the foliation and has an en echelon geometry (Fig. 6d). Late structures such as kink bands and faults are sometimes recognized crosscutting the former structures, both sharing a general N–S trend (Fig. 6e).

Relationship to the intrusive bodies

Granitoids that intrude the Rocha Formation cross-cut F_2 structures. On the other hand, no structures indicative of syn-deformation emplacement were recognized in

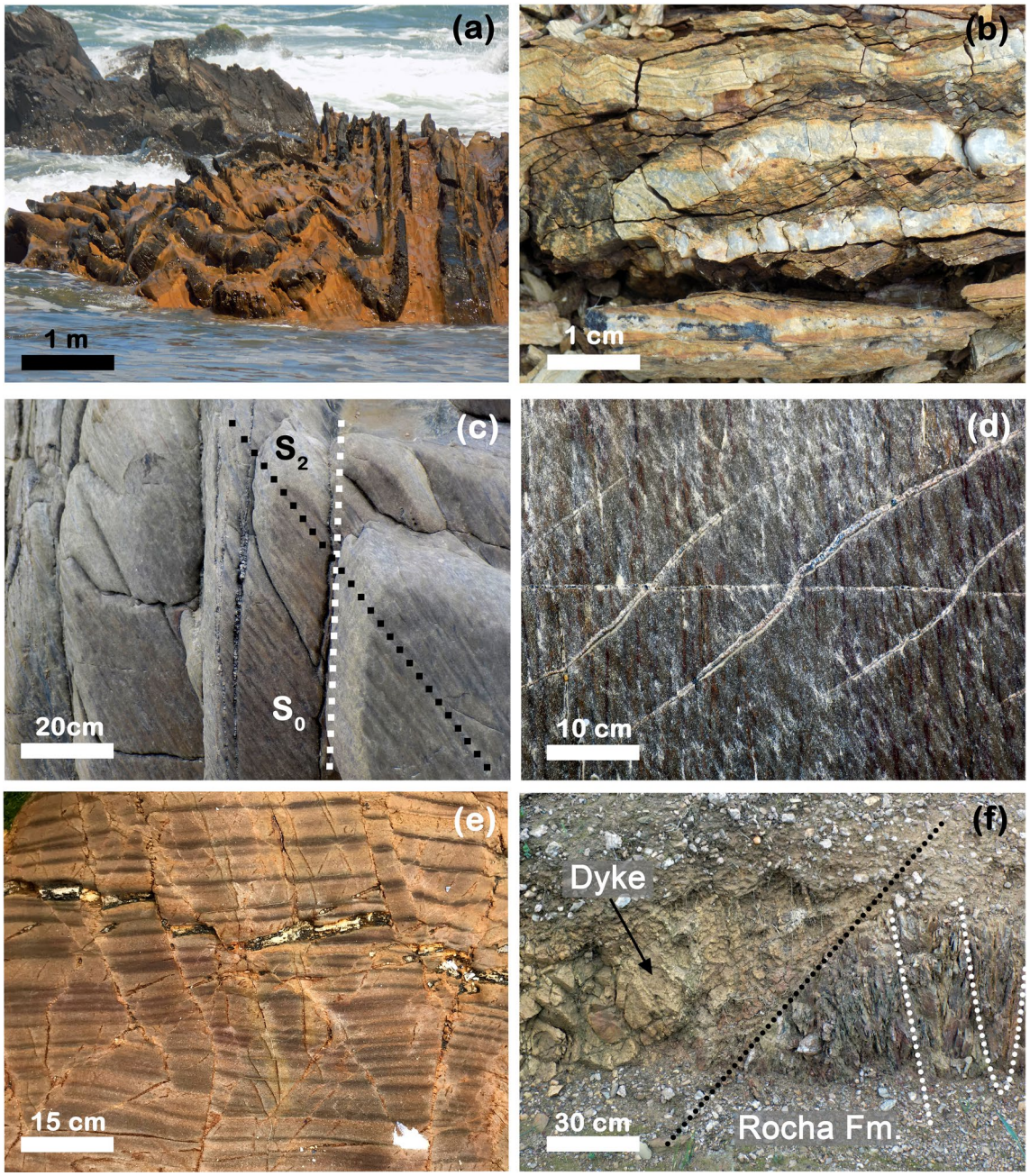

Fig. 6 Structural features of the Rocha Formation: **a** folds of the F_2 in metasandstones (dark layers) intercalated within metapelites; **b** isoclinal fold in metapelites (F_1), the middle band is a quartz vein folded together with the layers; **c** angular relationship between the cleavage and the bedding; **d** late *En Echelon* veins in metasandstones; e) Faulted metapelites; **f** structural relationship between the dacitic dyke dated in this work (UYS-06–18) and the F_2 of the Rocha Formation

the granites. Skarns are observed in the contact aureoles, showing a variable extension, with assemblages characterized by garnet + biotite + muscovite, biotite + chlorite, and chlorite + actinolite. In addition, a series of undeformed dacitic dykes were recognized discordantly cross-cutting the F_2 of the Rocha Formation (Fig. 6f), with a 045°–030° strike and variable dip/dip direction. They show a thickness of 1–15 m, and a maximum length of 3 km. They are porphyritic, with millimetric phenocrysts of quartz sometimes showing embayed structures, plagioclase and muscovite, and a matrix composed of fine-grained quartz and feldspar with sericitic alteration.

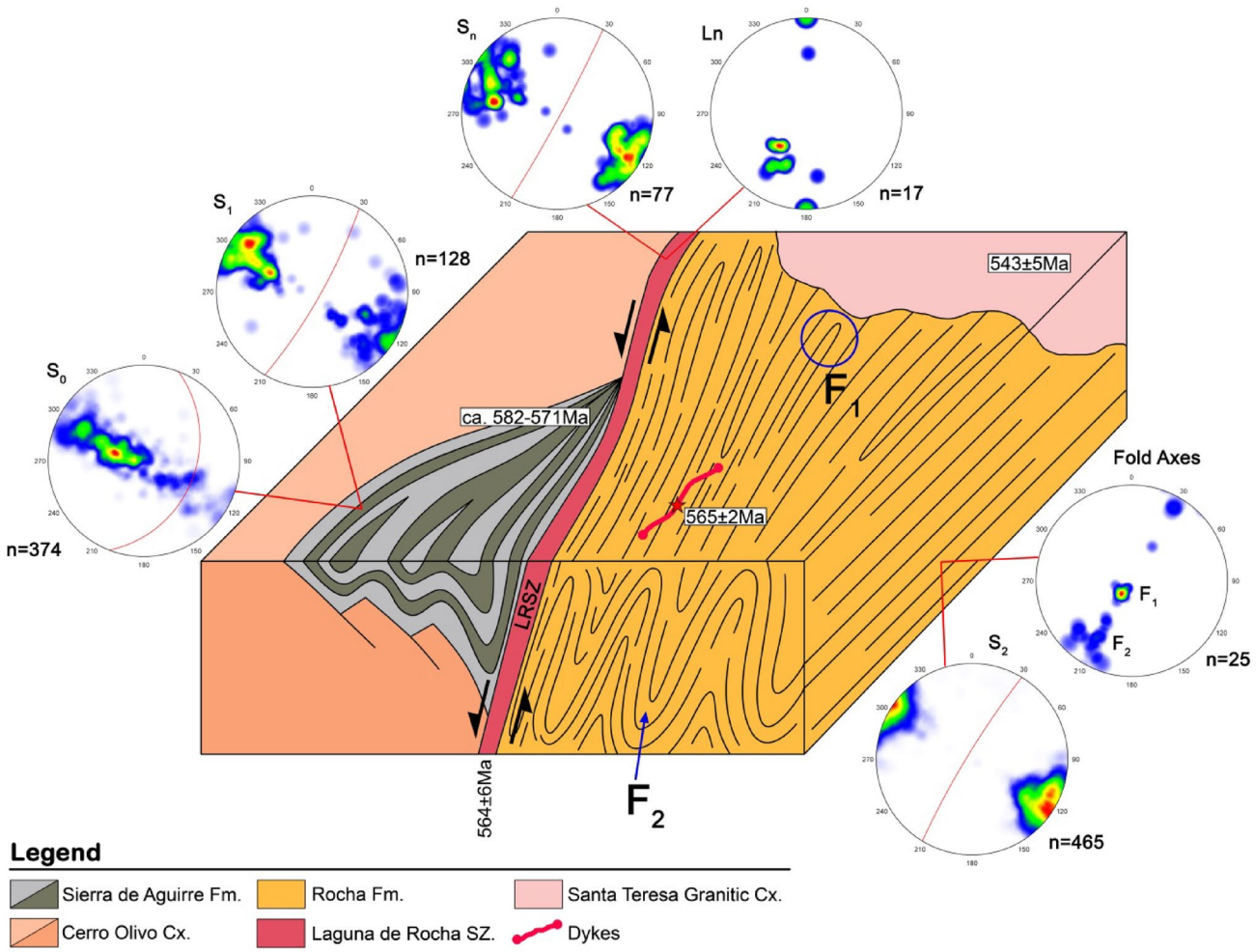

Fig. 7 Structural sketch of the Sierra de Aguirre region, between the approximate coordinates (34°00′S, 54°00′W) and (34°15′S, 54°10 W), showing the geometrical relation between the Sierra de Aguirre and Rocha Formations. The sketch also shows the structural data for both units and the Laguna de Rocha Shear Zone (Modified after Silva Lara et al. 2021)

Metamorphic grade and microstructures

The metamorphic grade of the sequence is low, with muscovite as the main metamorphic mineral constituting the cleavage (Fig. 4). In the proximity of the Laguna de Rocha Shear Zone, the mineral assemblages in the metasediments are dominated by chlorite, and a ductile behavior of quartz is characterized by bulging and sub-grain rotation. Similar observations have been made on the neighboring Sierra de Aguirre Formation on the other side of the same shear zone (Silva Lara et al. 2021). The occurrence of biotite as a metamorphic mineral, described by Betucci and Burgueño (1993), was not corroborated.

The S_2 cleavage shows different characteristics, directly related to the grain size and the amount of matrix in the case of the metasandstones. The coarser-grained and matrix-poor sandstones show a less developed cleavage, which is irregular and discontinuous, whereas fine-grained metasandstones and metapelites show parallel and well-developed cleavage (Fig. 4a, b). The main mineral that constitutes the cleavage is fine- to medium-grained muscovite, which is accompanied by minor chlorite. Sometimes the cleavage also has important amounts of fine-grained opaque minerals, suggesting pressure-solution processes.

Quartz veins related to pressure-solution processes are common in the Rocha Formation. They are commonly boudinated and parallel to the cleavage, with dynamic recrystallization of quartz dominated by bulging (Fig. 4e). Some quartz clasts are stretched with the major axis parallel to the cleavage. The presence of calcite patches within the metasandstones is common in the northern portion of the formation. These calcite grains show type I and II twins (Bukhard 1993) and less frequently bent twins. All microstructures observed in the metasediments suggest that deformation was active under temperatures below 400 °C, which is in accordance with the observed lower greenschist facies.

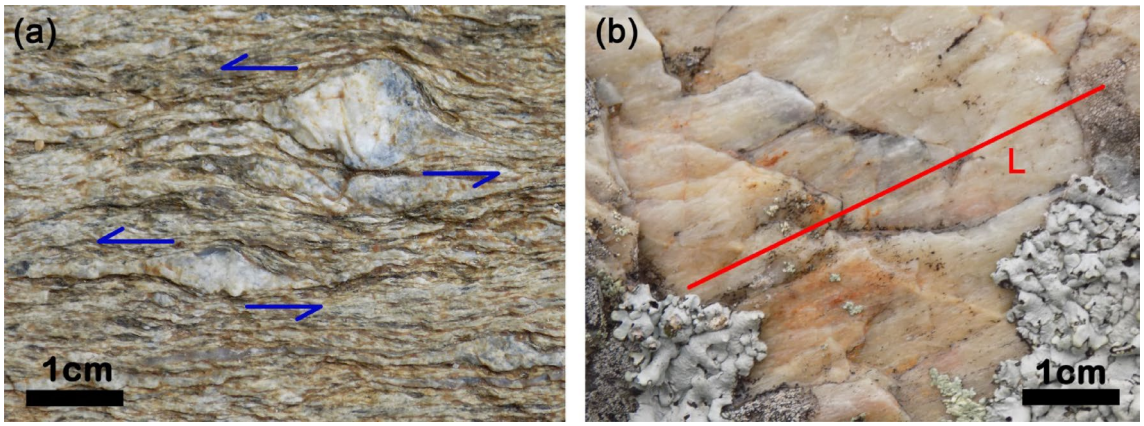

Fig. 8 **a** Gneissic mylonite of the Laguna de Rocha Shear Zone showing sinistral kinematic indicators, looking down, top to the north; **b** Quartz stretching lineation within quartz mylonites of the Laguna de Rocha Shear Zone, approximately N–S lateral view, lineation dipping to the SW

Laguna de Rocha Shear Zone

The Laguna de Rocha Shear Zone is the tectonic contact between the Cerro Olivo Complex and the Rocha Formation. Associated with this tectonic contact is a restricted basin, where the Sierra de Aguirre Formation is deposited. This shear zone has a general NNE–SSW trend, and a sinistral shear sense (Silva Lara et al. 2021, Fig. 8a). It dips steeply to the W in its western portion and variably to the W and the E in the eastern portion. A stretching lineation of quartz and fine-grained white mica was recognized (Fig. 8b), varying from horizontal to plunging around 45° to SSW (Fig. 7). Four types of mylonites were recognized: (a) chlorite-rich mylonites: this lithology is the most common within the shear zone, representing mylonitized schists of the Rocha Formation. Strongly stretched quartz veins are common; (b) quartz mylonites: this lithology crops out mostly in the contact between the Sierra de Aguirre and the Rocha Formation, particularly on the southern portion of the first. It is composed mostly of quartz, with variable amounts of muscovite/chlorite, which determines the mylonitic foliation; (c) mylonitic metasandstones: fine-grained gray rocks, rich in deformed quartz veins and with common isoclinal folds; and (d) granitic and gneissic mylonites: they show porphyroclasts of quartz-feldspar aggregates and a fine-grained matrix composed of quartz, muscovite, biotite and feldspar (Fig. 8a).

Samples

A total of 11 samples were analyzed, 4 belonging to the Cerro Olivo Complex, 5 to the Rocha Formation and 2 to the intrusive bodies. The key information of the samples is shown in Table 1, and an extended description in the supplementary material.

Table 1 Sample list

Name	Rock type	Unit	Technique/analysis
UY-01–16	Metapelite	Rocha Formation	U–Pb (LA-ICP-MS)/Lu–Hf/Sm–Nd
UY-03–16	Metapelite	Rocha Formation	Sm–Nd
UY-05–16	Metapelite	Rocha Formation	U–Pb (LA-ICP-MS)/Lu–Hf/Sm–Nd
UY-07–16	Metapelite	Rocha Formation	U–Pb (LA-ICP-MS)
UY-53–16	Metasandstone	Rocha Formation	U–Pb (LA-ICP-MS)
UY-12–16	Orthogneiss	Cerro Olivo Complex	U–Pb (SHRIMP)/Lu–Hf
UY-13–16	Orthogneiss	Cerro Olivo Complex	U–Pb (SHRIMP)/Lu–Hf
UY-14–16	Metaquartzite	Cerro Olivo Complex	U–Pb (LA-ICP-MS)/Lu–Hf
UY-15–16	Metaquartzite	Cerro Olivo Complex	U–Pb (LA-ICP-MS)/Lu–Hf
UY-19–16	Paragneiss	Cerro Olivo Complex	U–Pb (LA-ICP-MS)
UY-06–18	Dacite	Dyke	U–Pb (SHRIMP)
UY-16–16	Granite	Rocha Granite	U–Pb (LA-ICP-MS)

Analytical results

Geochronology of the Cerro Olivo Orthogneisses

Sample UY-12–16 (Orthogneiss)—The zircon grains of the sample are elongated and show regular to well-formed bipyramidal terminations. Oscillatory zoning patterns are a common feature. Most grains show overgrowths with homogeneous textures, and also sometimes homogeneous cores with a stubby geometry. Of the 17 analyzed spots, 15 produced < 10% discordant ages, out of which 6 outlying young ages were interpreted as Pb-loss and discarded from the age calculations. An individual U–Pb age yielding a result of 846 ± 16 Ma is interpreted as inherited. From the remaining spots, two ages were obtained. A concordia age of 773.3 ± 6.7 Ma (95% confidence, MSWD = 0.27, probability of concordance = 0.60), based on four spots measured on the cores of the grains with a magmatic structure, is interpreted as representative of the magmatic crystallization age of the rock. From the other four spots, measured on the rims and cores of homogeneous grains, a concordia age of 650.1 ± 5.2 Ma (95% confidence, MSWD = 0.083, probability of concordance = 0.77) is interpreted as the age of the metamorphic event under granulite facies conditions (Fig. 9a, b).

Sample UY-13–16 (Paleosome in migmatite)—The zircon grains of this sample show elongated to stubby shapes, with lengths between 250 and 120 µm. Bipyramidal terminations and magmatic zonings are developed in parts of the grains. Broken grains are common. Wide zircon overgrowths are absent, and for that reason the majority of the measurements were performed within the cores of the grains. All 12 analyzed spots produced concordant results, but due to a relatively large range of ages covered between the oldest and the youngest result (ca. 25 My), the mean $^{206}Pb/^{238}U$ ages were used as a guide to choose the best-defined population to calculate a concordia age of 781.9 ± 3.2 Ma (95% confidence, MSWD = 1.3, probability of concordance = 0.26), based on ten grains. This age is interpreted as the time of magmatic crystallization of the igneous protolith (Fig. 9c).

Detrital zircon results

The Cerro Olivo Paragneisses

Sample UY-14–16 (Metaquartzite)—The zircon grains of this sample have a size of 50–150 µm and are mostly stubby or fragments of larger crystals. Rounded shapes as well as overgrowths with homogeneous texture are common features. The main characteristics within the cores of the grains are complex oscillatory zoning. Seventy-five analyzed crystals produced concordant results, ranging from 663 to 1924 Ma (Fig. 10). The youngest observed peak is centered at 673 Ma ($n = 3$), and is interpreted as the age of metamorphism of the paragneiss. The remaining peaks represent main age populations in the Tonian (850–750 Ma, $n = 16$), Mesoproterozoic (1.3–1.0 Ga, $n = 46$) and late Paleoproterozoic (1.7 Ga; $n = 11$).

Sample UY-15–16 (Metaquartzite)—The zircon grains of this sample are rounded and have a size of 70–130 µm. The cores of the grains are fragments of larger crystals, either stubby or elongated, with oscillatory zoning, while the rounded overgrowths have a homogenous texture. From this sample, 96 spot analyses produced concordant results ranging from 707 to 1841 Ma (Fig. 10), with the youngest age peak centered at an age of 716 Ma ($n = 5$). The remaining peaks represent age populations in the Tonian (900–790 Ma, $n = 15$), Mesoproterozoic (1.4–1.0 Ga, $n = 55$) and Late Paleoproterozoic (1.7 Ga, $n = 6$).

Sample UY-19–16 (Paragneiss)—From this sample a total of 58 concordant results were obtained in different zircon crystals, ranging from 2909 to 643 Ma (Fig. 10). The youngest peak yielded an age of 652 Ma ($n = 12$), followed by significant populations in the Tonian (930–770 Ma, $n = 25$); Mesoproterozoic (1.1–1.0 Ga, $n = 6$), and Paleoproterozoic (1.8 Ga; $n = 3$).

The Rocha formation

Sample UY-01–16 (Fine-grained metapelite)—The analyzed detrital zircon grains are 50–200 µm long and mostly show prismatic shapes with oscillatory zoning. From this sample, 59 concordant results were obtained from different zircon crystals, with ages ranging from 1743 to 645 Ma (Fig. 10). The resulting ages show a near-unimodal distribution, with a main peak at 664 Ma ($n = 43$), and a subordinated Tonian peak (867–771 Ma, $n = 6$).

Sample UY-05–16 (Laminated Metapelite)—The analyzed detrital zircon grains are prismatic and 50–150 µm long. They exhibit oscillatory zoning as their main feature. Rounded grains, broken grains and grains with patchy textures or inclusions also occur within the sample. Fifty-four crystals from this sample produced concordant results, with ages ranging from 2435 to 661 Ma (Fig. 10). The youngest age peak of this sample is centered at 668 Ma ($n = 12$), with subsequent age peaks in the Tonian (821–722 Ma; $n = 26$) and Mesoproterozoic (1.0 Ga, $n = 6$), accompanied by grains yielding disperse Meso- to Paleoproterozoic individual ages.

Sample UY-07–16 (Fine-grained metapelite)—Only three grains of this sample were recovered, yielding concordant individual ages of 657, 696 and 2064 Ma (LA-ICP-MS). These ages will be added to the compilation of all the results of detrital zircons obtained for the Rocha Formation in the discussion.

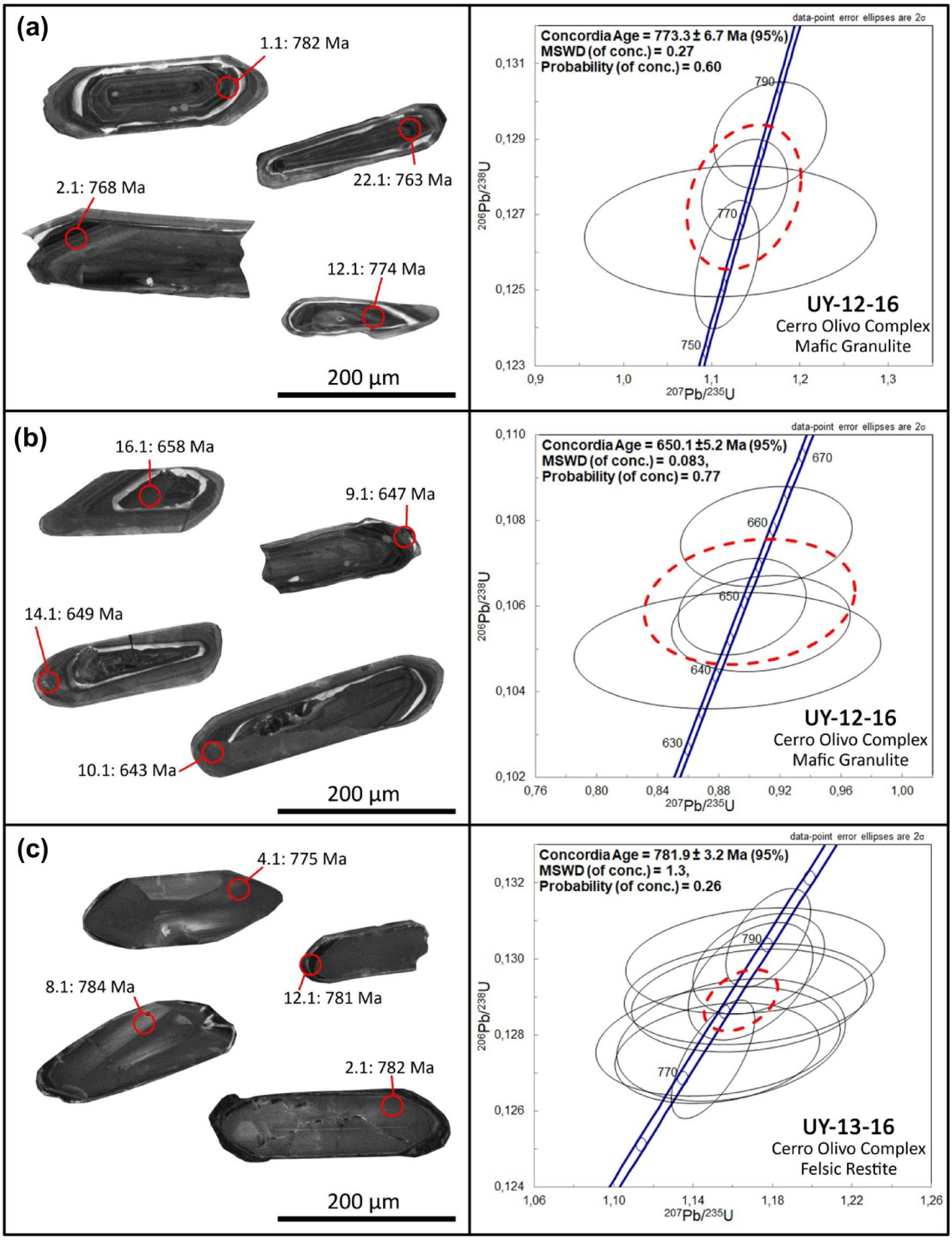

Fig. 9 Left side: Cathodoluminescence images of representative zircon grains and U–Pb concordia plots for samples dated from the Cerro Olivo orthogneisses. Right side: Concordia diagrams showing the individual results used to calculate the age. The red ellipses represent the concordia age, the black ellipses the grains employed to calculate the concordia age. Error ellipses are plotted at the 2σ level. MSWD: mean square of weighted deviates

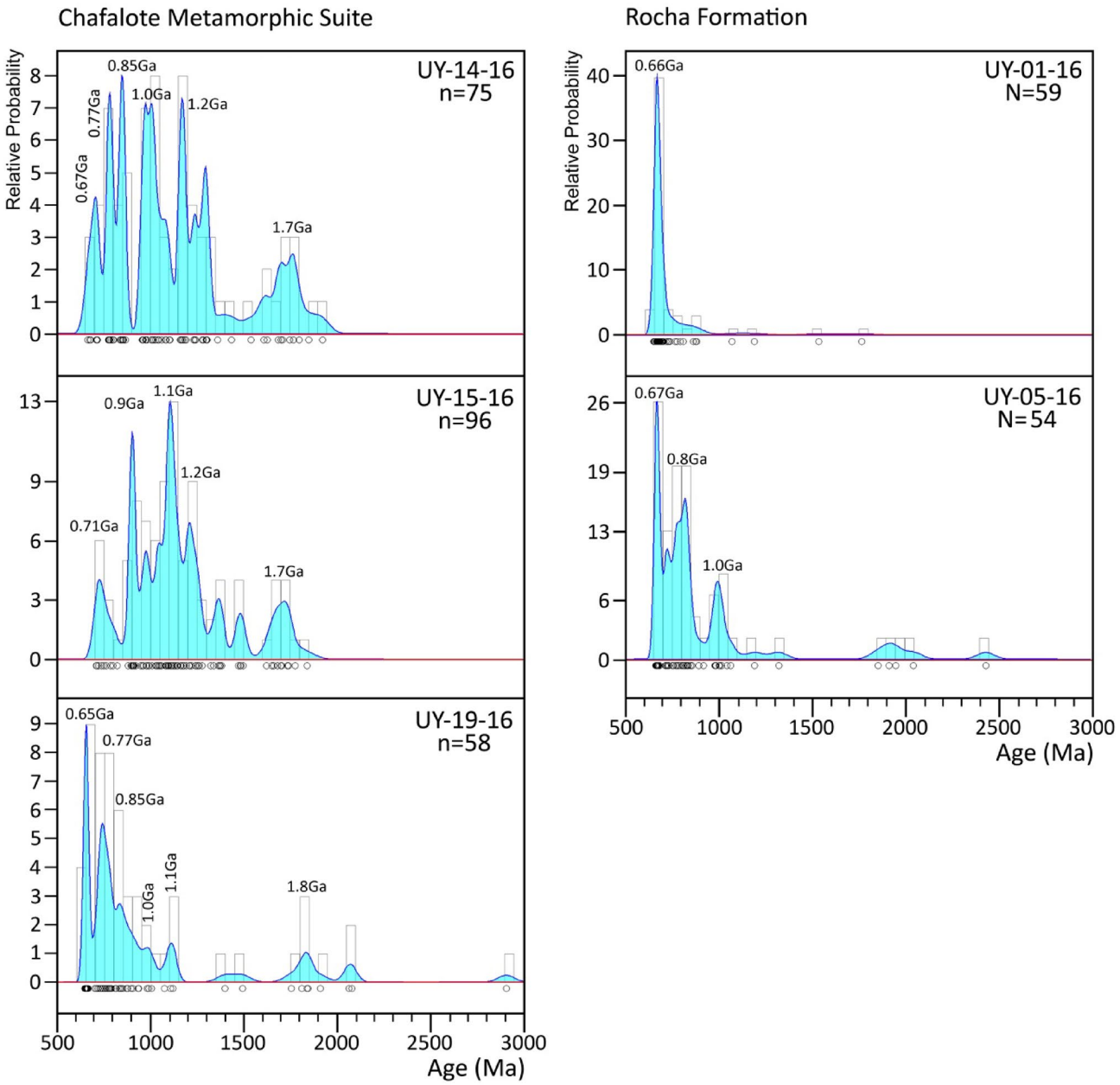

Fig. 10 Kernel density plots of detrital zircon age data for samples of the Chafalote Metamorphic Suite and the Rocha Formation (Bin width = 50 Ma)

Sample UY-53–18 (Fine-grained metasandstone)—Only ten detrital zircon grains from this sample were recovered, with ages ranging from 1999 to 604 Ma. As in the case of the former sample, these results will be added to the compilation of detrital zircon ages in the discussion.

U–Pb geochronology of the Ediacaran magmatic rocks

Sample UY-06–18 (Dacitic dyke intrusive to the Rocha Formation)—Zircon grains belonging to this sample have a variable grain size between 70 and 350 µm. They mostly

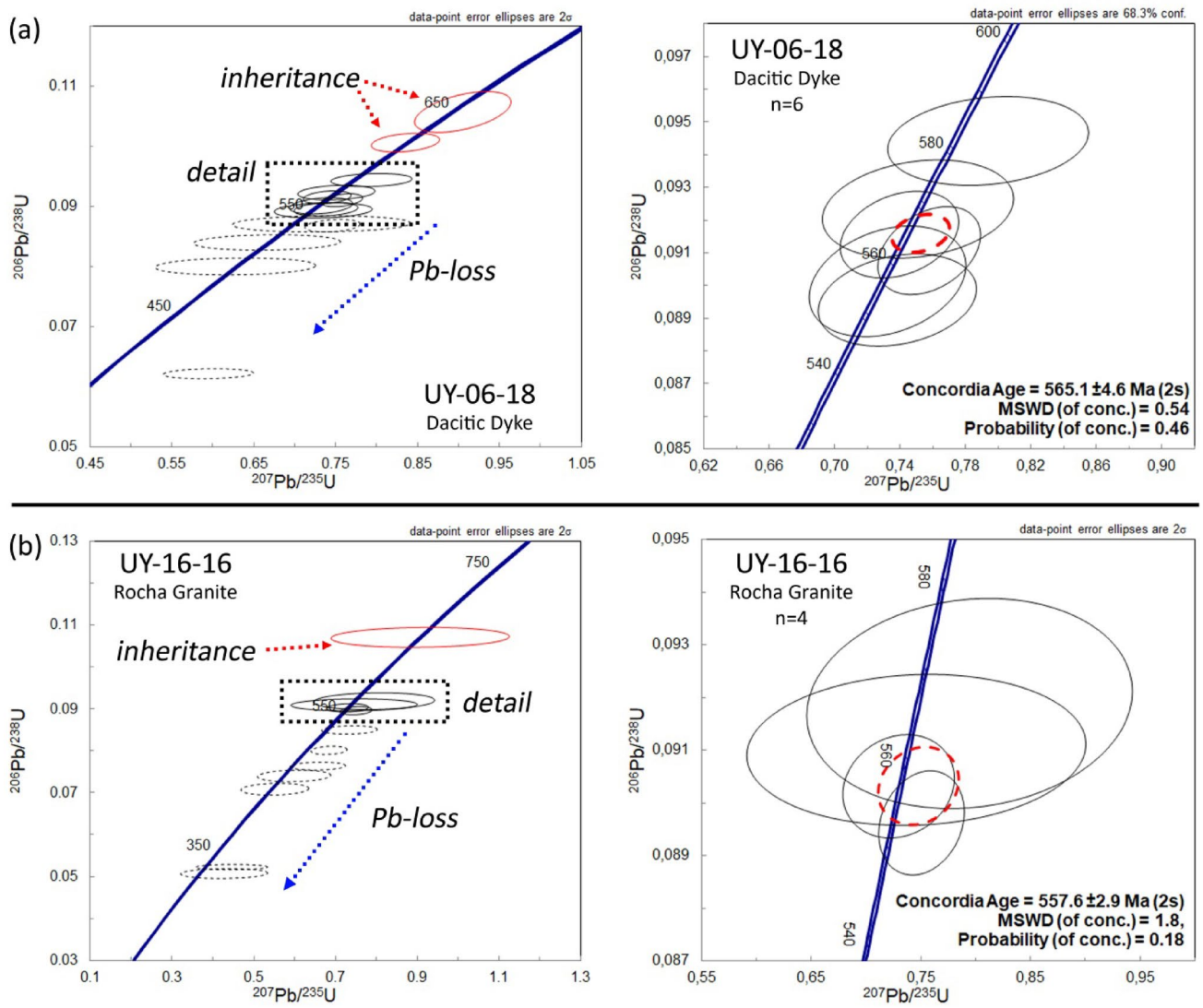

Fig. 11 Concordia diagrams for analyzed zircons from samples belonging to the Ediacaran magmatism of the Punta del Este Terrane. Left diagrams: red ellipses represent the inherited grains, black ellipses the grains employed to calculate the concordia age, and the dotted black ellipses represent Pb-loss. Right diagrams: the dotted red circles represent the calculated concordia age. **a** Sample UY-06–18, dacitic dyke; **b** Sample UY-16–16, Rocha granite

show prismatic elongated shapes, with bipyramidal terminations and oscillatory zoning. Some grains are broken or show cores with complex zoning. Out of the 14 analyzed spots, 11 produced < 10% discordant ages. Of these, three outlying young ages were discarded for the calculations, and interpreted as the result of Pb-loss. From the remaining points a concordia age of 565.1 ± 4.6 Ma was calculated (2σ, MSWD = 0.54, probability of concordance = 0.46), and interpreted as representative of the magmatic crystallization age of the sample (Fig. 11a). Two concordant grains yielding individual $^{206}Pb/^{238}U$ ages of 618 Ma and 648 Ma are interpreted as inherited.

Sample UY-16–16 (Rocha Granite—syn-kinematic to the Cordillera Shear Zone)—The zircon grains belonging to this sample are elongated and prismatic, with a size of 80–300 µm. They commonly show oscillatory zoning patterns, and broken

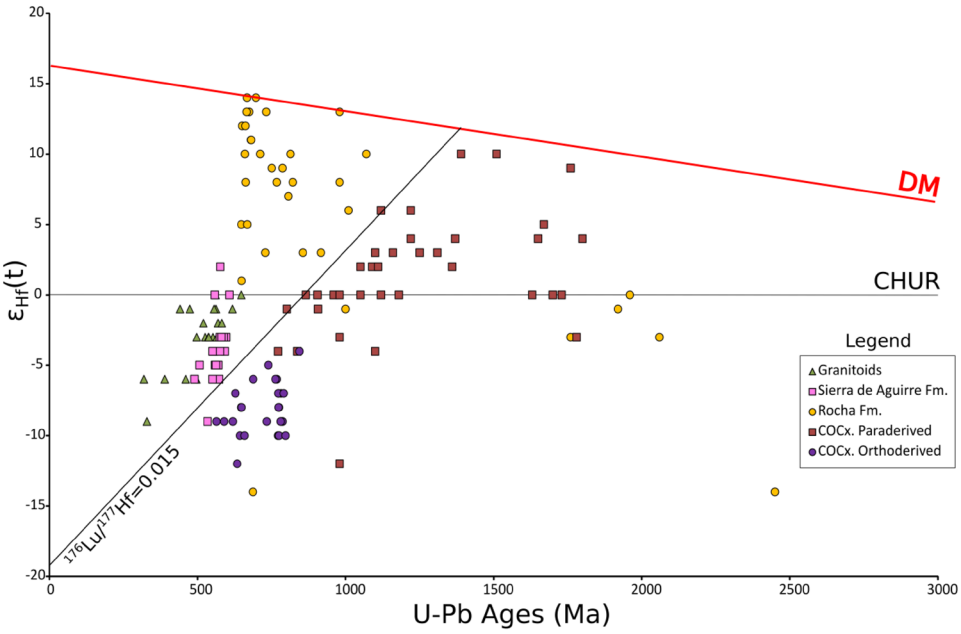

Fig. 12 New U–Pb versus εHf zircon data for the Cerro Olivo Complex, Ediacaran granitoids intrusive in the Punta del Este Terrane, and the Rocha Formation. Data of the Sierra de Aguirre Formation from Silva Lara et al. (2021)

terminations and crystal fragments are also common. From the 12 analyzed spots, only four gave < 10% discordant ages. From those points, two of them produced outlying $^{206}Pb/^{238}U$ individual ages. The younger individual outlying age of 441.4 ± 6.9 Ma was interpreted as the result of Pb-loss, and the oldest outlying age of 656.0 ± 11.3 Ma was interpreted as inherited. The remaining two concordant results were combined with two of the less discordant measured spots (< 20%), resulting in a concordia age of 557.6 ± 2.9 Ma (2σ, MSWD = 1.8, probability of concordance = 0.18) that is interpreted as the timing of the magmatic crystallization of the rock (Fig. 11b).

Zircon Lu–Hf isotopes

The Cerro Olivo Complex

The two analyzed orthogneiss samples (UY-12–16 and UY-13–16) show relative homogeneous results, with $^{176}Hf/^{177}Hf_{(i)}$ values ranging from 0.28198 to 0.28216, $\varepsilon Hf_{(t)}$ from − 12 to − 4, and T_{DM} ages from 2.2 to 1.9 Ga. These values suggest a crustal signature for the magmatic protoliths of the gneisses (Fig. 12).

On the other hand, the analyzed zircon grains in the paragneiss samples (UY-14–16 and UY-15–16) show two populations with contrasting characteristics. Tonian grains with U–Pb ages of 980 to 772 Ma yield $^{176}Hf/^{177}Hf_{(i)}$ values between 0.2818 and 0.28223, corresponding to slightly negative εHf(t) values between 0 and − 12 and Paleoproterozoic model ages (T_{DM} from 2400 to 1700 Ma). In contrast, zircon grains yielding Meso- and Paleoproterozoic U–Pb ages show $^{176}Hf/^{177}Hf_{(i)}$ values from 0.28169 to 0.28225, predominantly slightly positive to positive $\varepsilon Hf_{(t)}$ values from 0 to 10 (except for two grains with negative values), and Paleoproterozoic to Neoarchean model ages (T_{DM} 2600–1600 Ma). The characteristics of the Tonian zircon grains point to a source with a more pronounced crustal signature, while the Meso to Paleoproterozoic zircon grains seem to be related with a dominantly juvenile source.

The Rocha formation

Lu–Hf data were obtained in zircons from two samples of the Rocha Formation (UY-01–16 and UY-05–16) to complement the regional whole-rock Sm–Nd database. The analyzed zircon crystals have $^{176}Hf/^{177}Hf_{(i)}$ values ranging from 0.28079 to 0.28276, showing a distribution in two groups of $\varepsilon Hf_{(t)}$ values, depending on the individual U–Pb ages of the crystals: Neoproterozoic zircon grains show positive to strongly positive values, ranging from 1 to 14, while zircon grains yielding Paleoproterozoic U–Pb individual ages show slightly negative to negative values, from 0 to − 14 (Fig. 12). T_{DM} ages also show a similar contrast: Neoproterozoic zircon grains show either Neoproterozoic or Mesoproterozoic model ages, while model ages for the Paleoproterozoic grains are Neo- to Paleoarchean.

Whole-rock Sm–Nd isotopes of the Rocha formation

The isotopic whole-rock Sm–Nd ratios of three samples from the Rocha Formation were analyzed (UY-01–16, UY-03–16 and UY-05–16). Results are shown in Fig. 13 and listed in Appendix D. The samples show $\varepsilon Nd_{(600)}$ values between

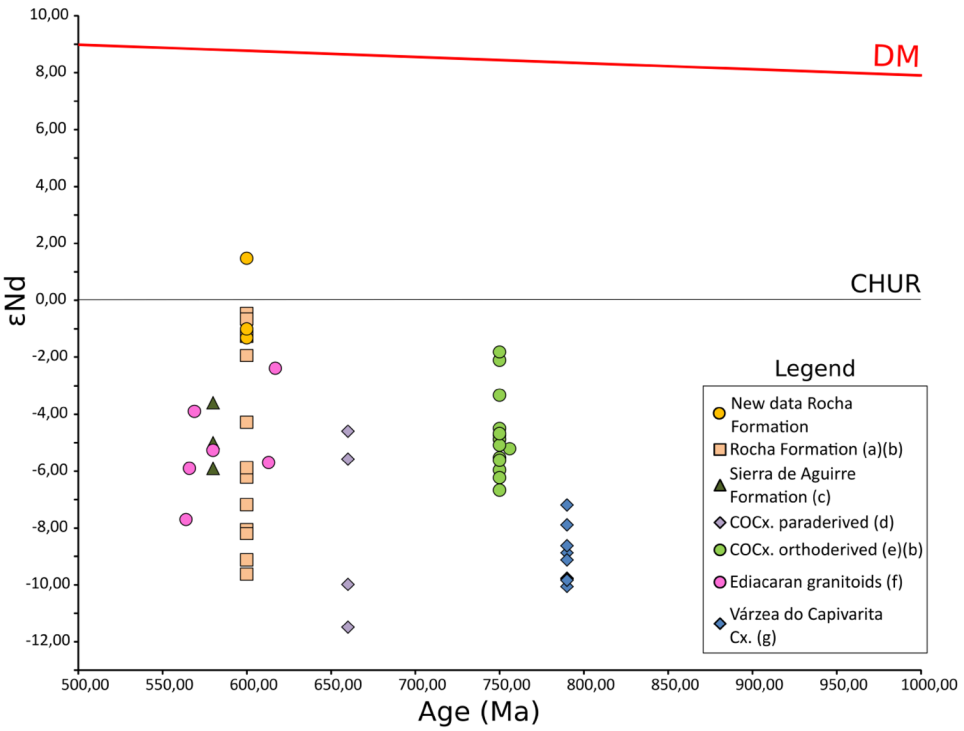

Fig. 13 U–Pb versus εNd data for different units of the Punta del Este terrane. Data from: **a** Abre et al. (2020), **b** Oyhantçabal et al. (2011), **c** Silva Lara et al. (2021), **d** Vieira et al. (2019), **e** Lenz et al. (2011), **f** Lara et al. (2020), **g** Martil et al. (2017)

− 1.32 and 1.47, whereas T_{DM} model ages are between 1.30 and 1.52 Ga.

Discussion

The Cerro Olivo Complex: origin and setting

Orthoderived rocks

Conflicting tectonic interpretations like rifting or a continental arc have been proposed for the Cerro Olivo Complex, mostly based on geochemical characteristics (Basei et al. 2010; Masquelin et al. 2012; Lenz et al. 2012; Koester et al. 2016; Konopasek et al. 2017; Martil et al. 2017; Tambara et al. 2019; Will et al. 2019; De Toni et al. 2021). Though not conclusive, the geochemical compositions show several characteristics suggestive of an arc setting, such as the general tonalitic–granodioritic nature of the rocks, moderate to high Ba, moderate to low Nb, the REE patterns and contents (ΣREE = 186 ppm in average), Ce_N (mean = 90), Ce_N/Yb_N (mean = 9), and La_N/Yb_N (mean = 11) values, as well as the average slightly negative to negative Eu anomalies indicative of processes of plagioclase fractionation in the source and/or assimilation (i.e. Lenz et al. 2011; Martil et al. 2017). Furthermore, the presence of high-K calc-alkaline compositions in the complex is also indicative of magmas that had either interaction with mica-rich metasedimentary rocks (e.g. Patiño-Douce 1999), or magmas related with partial melting of metagranitic and metasedimentary sources (e.g. Brown 2013; Chappell and White 1992; Chappell et al. 2012; Frost and Frost 2011; Sawyer et al. 2011) or even magmas with a metasomatized mantle source (e.g. Kelemen et al. 1993; Pearce et al. 1990; Qin et al. 2018; Turner et al. 1996).

The newly reported crystallization and metamorphism ages in this study for the orthogneisses fall within the age span of the published ages of the Cerro Olivo Complex (Hartmann et al. 2002; Oyhantçabal et al. 2009; Lenz et al. 2011; Masquelin et al. 2012; Peel et al. 2018; Will et al. 2019), namely, 800–760 Ma for the magmatic stage of the complex and 660–650 Ma for the high-grade metamorphism. On the other hand, the new Lu–Hf isotopic compositions of the orthogneisses in the present study point to an important contribution of an older crust in the generation of the magmas, with negative εHf values between − 4 and − 12, and Paleoproterozoic T_{DM} ages between 1.9 and 2.2 Ma. These new εHf results are supported by previously obtained Sm–Nd data, with εNd between − 1.8 and − 6.7 and T_{DM} ages between 1.3 and 2.1 Ga (Lenz et al. 2010; Konopasek et al. 2017, Figs. 12, 13). This crustal signature has been previously interpreted as related to the assimilation/recycling of a Paleoproterozoic–Archean basement (Koester et al. 2016; Martil et al. 2017; Petrolli 2017; Hueck et al. 2022), but also due to the assimilation of sediments/supracrustal rocks (Will et al. 2019). Since there is no clear pre-Tonian basement related to the Cerro Olivo Complex, the participation of a non-outcropping or completely reworked basement is hard to explain but cannot be ruled out. Thus, this crustal

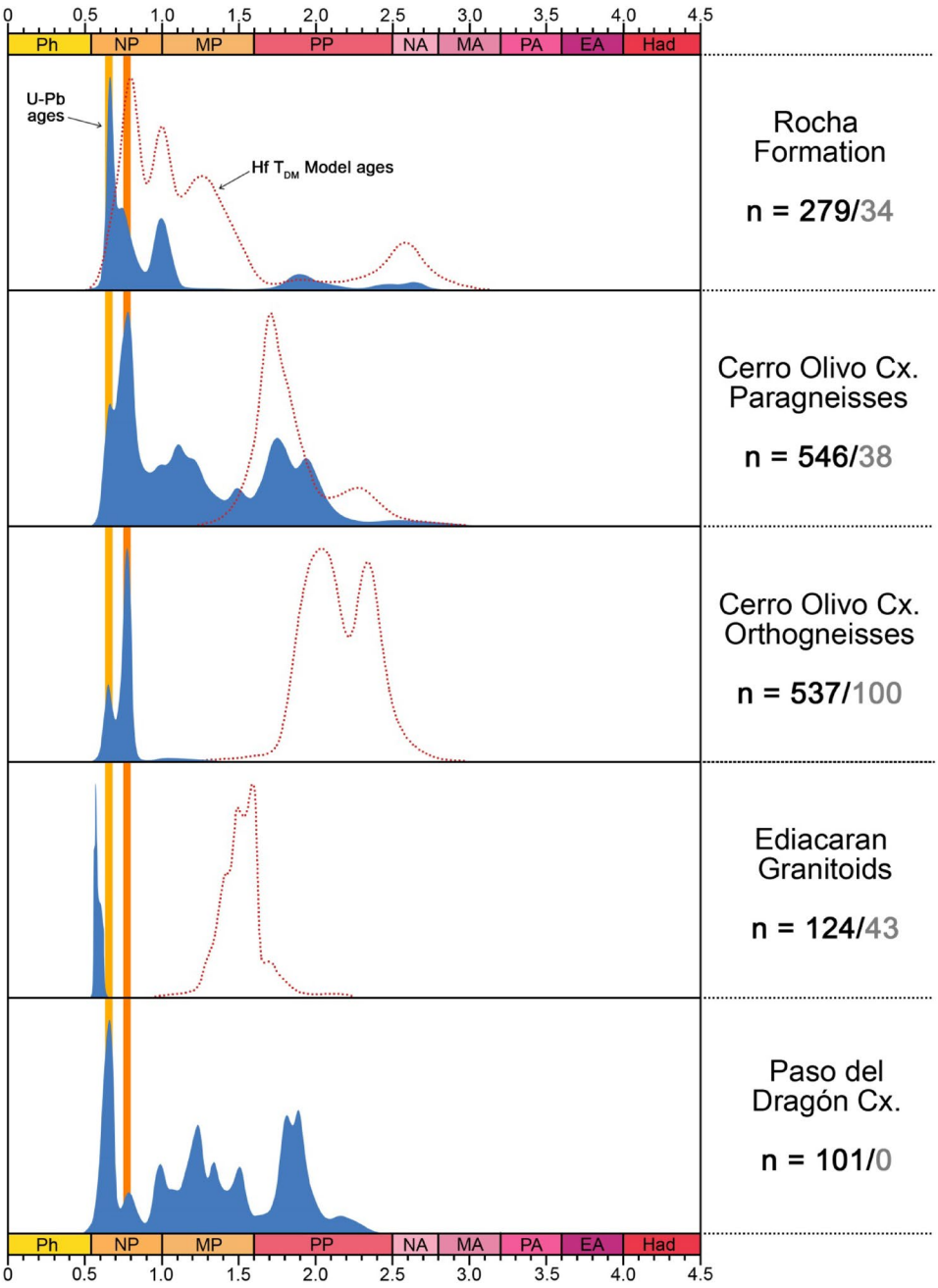

Fig. 14 Compilation of the available U–Pb individual zircon ages and Hf TDM model ages for the units of the Punta del Este Terrane. The light orange band represents the 630–670 Ma age span, and the dark orange line the 760–800 Ma span. Data from: the present study, Oyhantçabal et al. (2009), Lenz et al. (2011), Masquelin et al. (2012), Gaucher et al. (2014), Koester et al. (2016), Konopasek et al. (2017), Peel et al. (2018), Will et al. (2019), Abre et al. (2020), Lara et al. (2020), Vieira et al. (2019), Silva Lara et al. (2021) and De Toni et al. (2021)

component seems to be strongly influenced by the assimilation of sedimentary/metasedimentary rocks, which also accounts for the general geochemical fingerprint, the isotopic fingerprint of ortho- and paragneisses and previously reported structural relationships (Masquelin 1990, 2001, 2005; Masquelin et al. 2002, 2006; Preciozzi et al. 1993, 1999, 2002).

It has been suggested that melting of the Mesoproterozoic metabasic lithologies of the Nico Pérez Terrane with T_{DM} up to 1.8 Ga (Mallmann et al. 2007; Oriolo et al. 2019) could be the source of the Cerro Olivo Complex protoliths (Konopasek et al. 2017). However, these units are gabbros which show geochemical signatures coherent with an intraplate setting (Oriolo et al. 2019). If they were indeed the source of the magmatic protoliths of the Cerro Olivo Complex, the idea of an inherited arc-related geochemical signature for the complex, as proposed in Konopasek et al. (2017), seems to be contradictory. On the other hand, these metabasic units show crystallization ages of ca. 1.5 Ma (Oyhantçabal et al. 2005; Oriolo et al. 2019), considerably older as the dominant ages of inherited zircon crystals within the orthogneisses, namely 1.0–1.3 Ga (Lenz et al. 2011; Masquelin et al. 2012). These Late Mesoproterozoic ages are uncommon in the Nico Pérez Terrane, and, therefore, this terrane

is discarded as a source for the magmas of the orthogneisses of the Cerro Olivo Complex.

Paraderived rocks

Age distributions of detrital zircons from the paraderived rocks of the Cerro Olivo Complex, show main peaks at ca. 660–650 Ma and 800–770 Ma (Konopasek et al. 2017; Peel et al. 2018, this work, Figs. 10, 14), corresponding, respectively, to the metamorphic peak of the complex and the main magmatic stage recorded in the orthoderived rocks. Additional peaks at 1.0–1.3 Ga are younger than the known Mesoproterozoic ages of the Nico Pérez Terrane. Paleoproterozoic and particularly Archean populations, which correspond to the main signatures of the basement units of the Nico Pérez Terrane, are also proportionally much less common than in the metasedimentary cover sequences of the latter (Oyhantçabal et al. 2020 and references therein, Fig. 14).

On the other hand, one of the analyzed samples shows a peak at 716 Ma, an age between the main magmatism of the complex and the metamorphic peak. Equivalent ages have not been found in previous studies implying that younger sediments are also involved to some extent in this complex, in spite of the reported structural relationships between most ortho- and paragneisses. This age is difficult to assign to a certain source, but it could be related to the late stages of the magmatism in the São Gabriel Terrane, namely at ca. 720 Ma (e.g. Phillip et al. 2018).

Furthermore, isotopic signatures of detrital zircons yielding Neo- to late Paleoproterozoic U–Pb ages show dominantly positive εHf values and Meso- to Paleoproterozoic T_{DM} model ages (Figs. 12, 14), contrasting with known data for the cover successions of the Nico Pérez Terrane, where the Archean component is always well-represented and the εHf values of zircon yielding Neo- to Paleoproterozoic U–Pb ages are dominantly negative (Oyhantçabal et al. 2020 and references therein). Consequently, the Nico Pérez Terrane basement probably did not act as an important source area for the analyzed paragneisses of the Cerro Olivo Complex, in contrast with previous proposals (Konopasek et al. 2017).

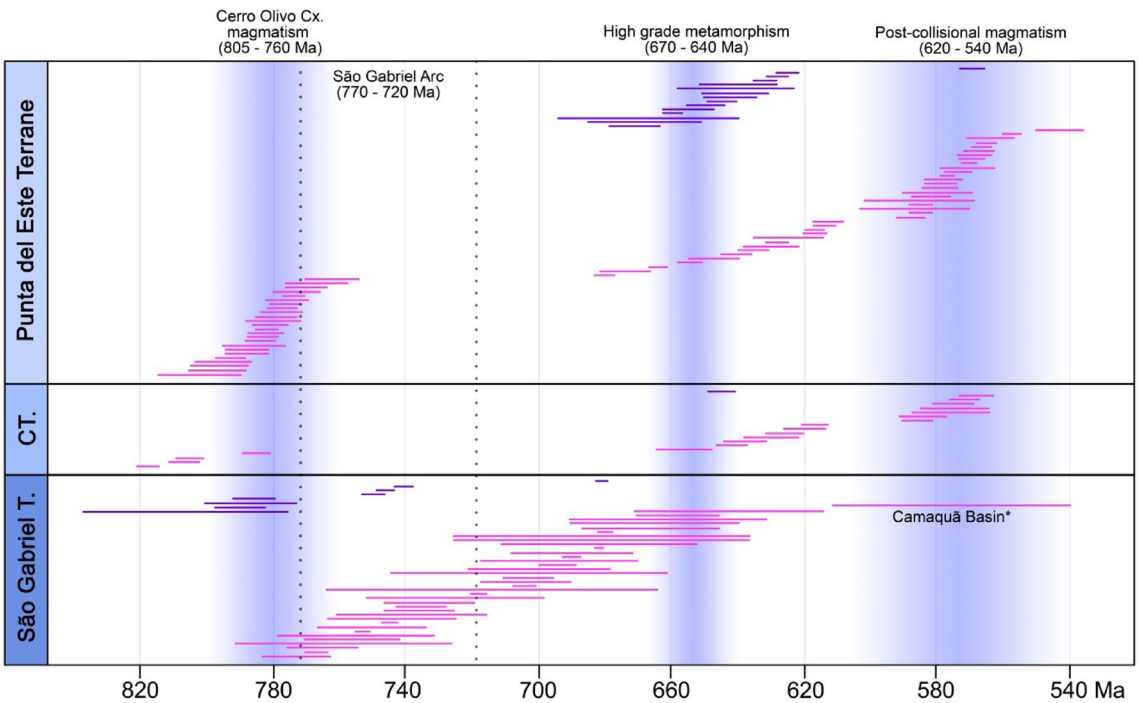

Fig. 15 Comparison between magmatic and metamorphic ages of the Punta del Este, Coastal and São Gabriel terranes. The pink error bars represent the magmatic ages and the violet ones the metamorphic ages. The ages of the Camaquã basin are represented as a single error bar to simplify the diagram. The data used for the Coastal and the Punta del Este terranes just comprise U–Pb ages and the data plotted for the São Gabriel Terrane include Sm–Nd ages (ages in mafic–ultramafic rocks). Data from: the present study, Cordani et al. (1973), Teixeira (1982), Soliani (1986), Silva and Soliani (1987), Machado et al. (1990), Remus (1991), Babinski et al. (1996), Franz et al. (1998), Leite et al. (1998), Remus et al. (1999), Seth et al. (1998), Silva et al. (1999), Basei et al. (2000, 2010, 2013), Hartmann et al. (2009, 20112002), Goscombe et al. (2005), Philipp et al. (2008, 2014), Konopasek et al. (2008, 2016, 2017), Oyhantçabal et al. (2009), Bongiolo et al. (2010), Bossi and Gaucher (2010), Lenz et al. (2011, 2014), Masquelin et al. (2012), Pecoits et al. (2012), Gaucher et al. (2014), Koester et al. (2016), Gubert et al. (2016), Peel et al. (2018), Klein et al (2018), Chaves Ramos et al (2018), Will et al. (2019), Tambara et al. (2019), Vieira et al. (2019), Lara et al. (2020), Ballivan Justiniano et al. (2020), and Silva Lara et al. (2021)

Relationship between ortho- and paragneisses and tectonic implications

In spite of the crustal signature of the Cerro Olivo Complex, there is no clear basement recognized for it, but some features point to metasedimentary rocks as an important source for this Tonian magmatism. The geochemical characteristics of the complex point to an arc-like setting, but with parameters suggesting that the sources of the magmatism were influenced by metasedimentary rocks, such as the high K_2O contents, and peraluminous compositions in the A/CNK vs. A/NK diagram (see i.e. Masquelin et al. 2012; Tambara et al. 2019). Similar inferences were postulated by Will et al. (2019), taking into account the Hf–O isotopic composition of zircons and whole-rock Nd fingerprint. Furthermore, the trend observed in the Lu–Hf values between ortho- and paragneisses, also suggest a process of assimilation of the metasedimentary rocks by the original magmas (Fig. 12).

On the other hand, the presence of a large Tonian peak in the detrital zircon spectra of the paragneisses, with a similar age to the main magmatic stage of the Cerro Olivo Complex is contradictory with a within plate scenario as suggested by previous authors (Basei et al. 2010; Konopasek et al. 2017; Will et al. 2019, 2021), in which zircon grains coeval to the extension are scarcely or not represented in the associated cover successions (Cawood et al. 2012). Furthermore, the mainly tonalitic–granodioritic nature of the complex is also unlikely in a rift setting, where a bimodal or mainly mafic magmatism would be expected.

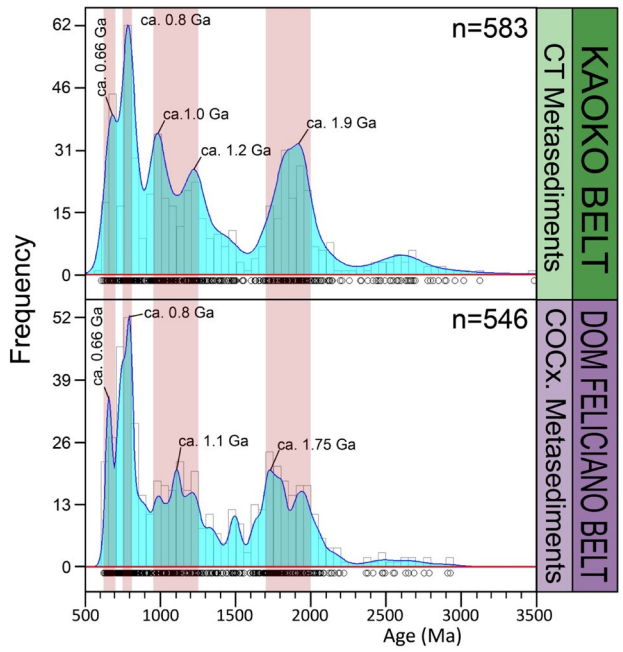

Fig. 16 Compared detrital zircon spectra of the paraderived rocks from the Punta del Este and Coastal terranes. COCx—Cerro Olivo Complex, CT—Coastal Terrane. Data from: the present study, Konopasek et al. (2014, 2017)

Lu–Hf results for the ortho- and paragneisses are dissimilar, with mostly positive εHf values for the Neo- to Paleoproterozoic zircons in the paragneisses, whereas the Neoproterozoic zircons of the orthogneisses are homogeneously negative. Since the known signatures for the Mesoproterozoic units of the Dom Feliciano Belt have a mix of crustal and mantellic signals, but with a tendency to crustal signals, it is suggested that these zircons have a distal source.

On the African side, very similar Tonian magmatic ages can also be found in the Coastal Terrane of the Kaoko Belt (Fig. 15, e.g. Kónopasek et al. 2008, 2017; Will et al. 2019). This correlation between both crustal blocks has already been envisaged not only based on the age spectra (e.g. Oyhantcabal et al. 2009; Kónopasek et al. 2017; Will et al. 2019), but also on the geochemistry of both, and is further supported by high-T/low-P granulite facies metamorphism at ca. 650 Ma (e.g. Goscombe and Grey 2007; Gross et al. 2009). When compared, detrital zircon spectra of the paraderived rocks of both blocks also show striking similarities, strengthening the already envisaged correlation between both blocks (Fig. 16). Furthermore, they also share a coeval Ediacaran granitic magmatism (e.g. Konopasek et al. 2005; Goscombe et al. 2005).

A possible alternative to reconcile apparently contradictory signatures of both, arc and rift settings, is an extensional arc, in a retreating accretionary orogeny. The geochemical characteristics of the orthogneisses, mainly arc-like, but with some extension characteristics as pointed out by Konopásek et al. (2017), could be explained by this setting. Results also indicate an important component of contamination related to the sediment assimilation, which may result from the mixing of these older crustal sources, with Tonian juvenile inputs, as proposed by Hueck et al. (2022).

This subduction scenario with upper plate extension can not only account for the particular signatures of the Cerro Olivo Complex, but also explains the presence of the partially coeval but very dissimilar São Gabriel Terrane (Fig. 17), which is characterized by Tonian magmatism dominated by juvenile mantle-derived contributions in an arc setting (e.g. Philipp et al. 2018; Hueck et al. 2022). An early subduction over the border of the Congo Craton, represented by the Punta del Este and Coastal Terrane might have resulted in localized crustal extension in the arc and back-arc domains, recorded within minor crustal fragments represented by the basement inliers of the Dom Feliciano Belt (Figs. 1, 17, see Hueck et al. 2022 for further details). Subduction led to the accretion of the São Gabriel juvenile association to the continental margin. This accretion is suggested as having occurred between 770 and 760 Ma, when magmatism in both blocks overlap in age (Figs. 16, 17).

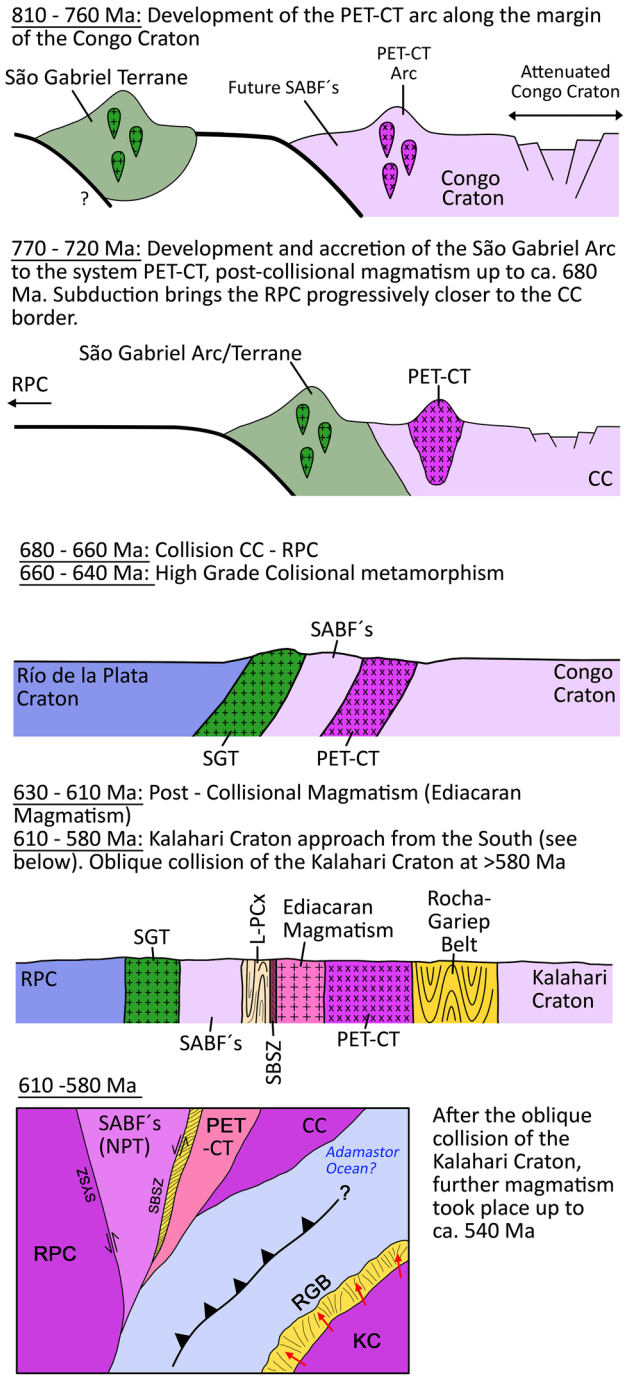

Fig. 17 Schematic model for the evolution of the Punta del Este terrane. SABF´s: South American Basement fragments, PET-CT: Punta del Este—Coastal Terrane, SGT: São Gabriel Terrane, RPC: Rio de la Plata Craton, L-PCx.: Lavalleja—Porongos Complex, CC: Congo Craton, KC: Kalahari Craton, RGB: Rocha—Gariep Belt, SBSZ: Sierra Ballena Shear Zone, SYSZ: Sarandí del Yí Shear Zone

Afterwards, further magmatism took place in the new active margin up to 720 Ma (e.g. Phillip et al. 2016, 2020; Hueck et al. 2022). Magmatism with post-collisional characteristics is found in both terranes from ca. 700 Ma up to ca. 680 Ma (e.g. Phillip et al. 2018; Vieira et al. 2019), but magmatic ages in felsic gneisses can be found in the Punta del Este Terrane up to the age of the main metamorphic peak, namely ca. 665 Ma (e.g. Gaucher et al. 2014), which probably represents the same magmatism.

The high-grade metamorphic event of the Cerro Olivo at ca. 660–640 Ma corresponds to the earliest record of the Brasiliano Orogeny in the Dom Feliciano Belt. The main phase of crustal shortening and high- to medium-grade metamorphism of the latter is constrained up to ca. 600 Ma, and was succeeded by sinistral shearing along orogen-parallel shear zones (Oriolo et al. 2016; Hueck et al. 2019; De Toni et al. 2021). Though some authors suggested a main phase of the deformation and metamorphism at ca. 550 Ma for the Dom Feliciano Belt (Frimmel 2010; Frimmel et al. 1998, 2002, 2011; Frimmel and Fölling 2003), these events are mainly recorded at the southeasternmost region (e.g. Rocha Formation) and temporally overlap with the final post-collisional magmatic and sedimentary processes of the Dom Feliciano Belt (e.g. Janikian 2004; Janikian et al. 2012; Basei et al. 2013; Matté et al. 2016; Sommer et al. 2011, 2017).

The Rocha Formation: sources and age constrains

The scarcely preserved primary sedimentary structures (Fig. 5), together with the dominantly pelitic deposits, are not enough to suggest a concrete depositional environment, being compatible with different depositional scenarios, from transitional fluvial to tidal plain (Basei et al. 2010). Features interpreted as related to turbidite deposits (Abre et al. 2020), mostly the cyclical arrangement of the bedding, are here interpreted as the result of structural repetition of the sequence due to folding. Nevertheless, a turbidite origin is not discarded.

The detrital zircon ages of the Rocha Formation are consistent between the samples, showing a main Neoproterozoic peak at ca. 660 Ma, with subordinated Tonian (ca. 0.8 Ga), Mesoproterozoic (ca. 1.0–1.1 Ga) and Paleoproterozoic peaks (ca. 1.8–2.0 Ga). These results are also consistent with those presented in previous studies (Basei et al. 2005; Abre et al. 2020), which also identified limited Neoarchean zircon grains (Figs. 10, 14). These detrital zircon spectra show a good correlation to the spectra of the Gariep Belt, particularly with the Oranjemund Group of the Marmora Terrane, which also lacks a large Paleoproterozoic peak (Fig. 18).

Most of the Neoproterozoic zircon grains show positive εHf values between + 1 and + 14, suggesting a juvenile source for them. This fact discards the Cerro Olivo Complex, particularly the orthogneisses characterized by negative εHf values, as a source for the Rocha Formation. On the other hand, the absence of grains recording the typical ages for the

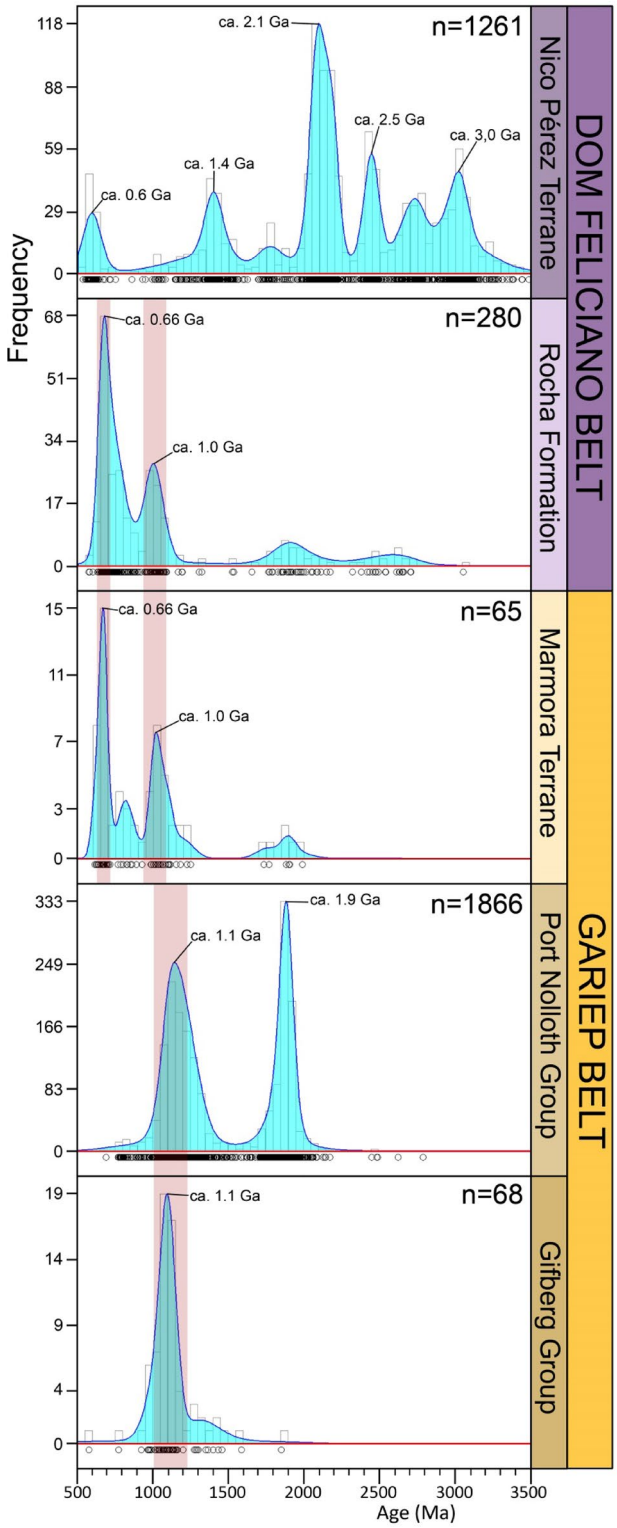

Fig. 18 Comparison between the detrital zircon spectra of the Gariep Belt, the Rocha Formation and the Nico Pérez Terrane. Data from: the present study, Basei et al. (2005), Hofmann et al. (2014, 2015), Konopasek et al. (2014, 2017), Naidoo et al. (2017), Andersen et al. (2018), and Abre et al. (2020)

voluminous and widespread Ediacaran granitic magmatism of the Dom Feliciano Belt (ca. 630–550 Ma), suggest that it was not involved as a source for this basin, though they may be coeval. Sm–Nd data and geochemical analyses (Basei et al. 2011; Abre et al. 2020) point to a juvenile input in the source of the Rocha Formation (Basei et al. 2011; Abre et al. 2020). To summarize, all the listed characteristics point to a source allochthonous to the Dom Feliciano Belt and its basement (e.g. Cerro Olivo Complex, Nico Pérez Terrane).

On the other hand, the isotopic signature and ages of the Kalahari Craton fit well with the new results reported here, suggesting that the Rocha Formation has a Kalahari affinity (Fig. 19, Oriolo and Beker 2018 and references therein). Particularly, the isotopic signatures of the Rocha Formation are coincident with those of the Oranjemund Group of the Marmora Terrane of the Gariep Belt (Fig. 19), reinforcing the already proposed link between both units (i.e. Basei et al. 2010; Abre et al. 2020). Therefore, the Rocha Formation is envisaged as a part of the Marmora Terrane of the Gariep Belt that was accreted to the Dom Feliciano Belt in the Ediacaran.

Folding geometries F_1 and F_2 show an interference pattern, where the F_2 folds re-fold the F_1 fold, thus, representing a progressive deformation. The F_2 folds show axial planes and fold axes, respectively, sub-parallel to the mylonitic foliation and stretching lineation observed in the Laguna de Rocha Shear Zone (Fig. 9). Together with the tightening of the folds on the proximity of the former, suggests that F_2 is related to the activity of the shear zone, as was previously interpreted for the neighboring Sierra de Aguirre Formation on the other side of the shear zone (Silva Lara et al. 2021).

The above mentioned Sierra de Aguirre Formation also represents an important age constraint for the Rocha Formation. Its deposition is directly associated with a restricted basin developed in association with the Laguna de Rocha Shear Zone, thus implying that the accretion between the Cerro Olivo Complex and the Rocha Formation happened prior to 582 Ma, an age of the youngest deposits of the Sierra de Aguirre Formation. This relationship is also supported by the fold geometries, recording the Sierra de Aguirre Formation the second folding phase of the Rocha Formation, but lacking in the first folding phase of the former. Based on this connection, the age of F_1, and, therefore, the age of the basin closure, is constrained between the age of the youngest deposits of the Rocha Formation, namely < 660 Ma, and the age of the age of the youngest deposits of the Sierra de Aguirre Formation (ca. 582 Ma, Silva Lara et al. 2021).

To constrain the age of the F_2, we need to take into account the age of the shearing of the Laguna de Rocha Shear Zone. As mentioned previously, this shear zone, as with most of the other shear zones of the belt, had a protracted evolution (e.g. Oyhantcabal et al. 2010, 2018; Oriolo et al. 2016; Hueck et al. 2018, 2019) since it was already

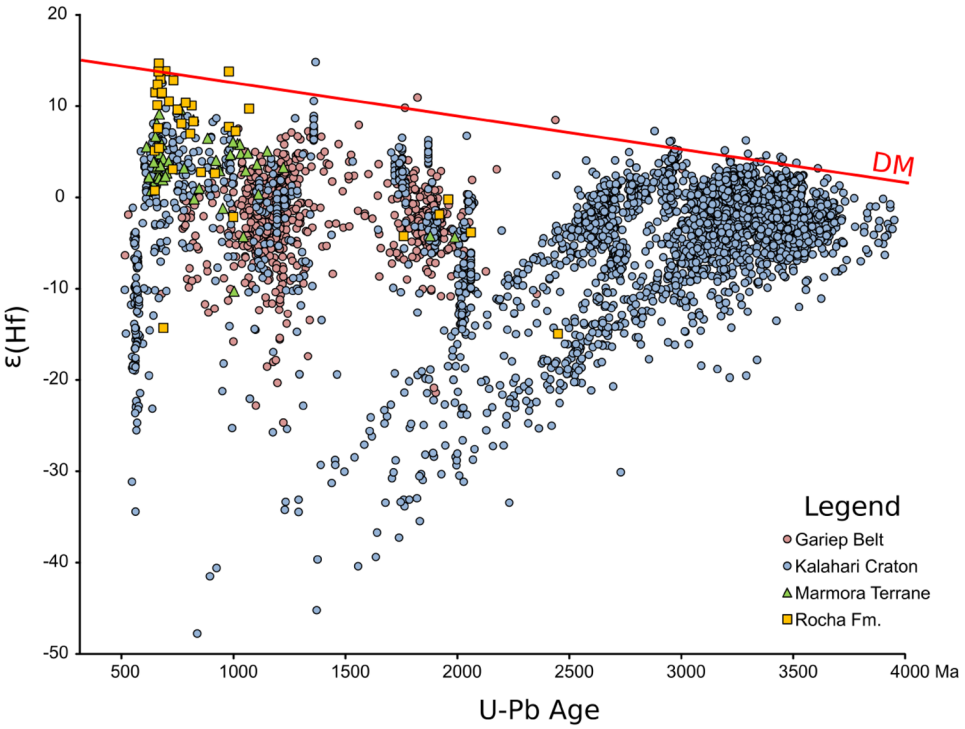

Fig. 19 Synthesis of εHf versus U–Pb zircon data of the Kalahari Craton, the Rocha Formation, the Gariep Belt and its Marmora Terrane ($n = 4395$; Basei et al. 2005; Zeh et al. 2007, 2008, 2009, 2010, 2011, 2013a, b, 2014; Zeh and Gerdes 2012; Frimmel et al. 2013; Foster et al. 2014; Hofmann et al. 2014, 2015; van Schijndel et al. 2014; Zirakparvar et al. 2014; Colliston et al. 2015; Cornell et al. 2015; Milani et al. 2015; Andersen et al. 2018; Abre et al. 2020). Data were recalculated considering a constant decay $\lambda\ ^{176}Lu = 1.867 \times 10^{-11}$ year^{-1} (Söderlund et al. 2004) and CHUR values of $^{176}Hf/^{177}Hf = 0.282772$ and $^{176}Lu/^{177}Hf = 0.0332$ (Blichert-Toft and Albarède 1997)

active prior to the deposition of the Sierra de Aguirre Formation (Silva Lara et al. 2021). The F_2 folds are sheared between the Rocha and the Sierra de Aguirre Formation, hence, the lower age constraint for the F_2 is given by the age of the youngest deposits of the volcanic succession, namely ca. 570 Ma. Afterwards a change in the dynamics of the shear zone led to the folding of both supracrustal sequences. The upper age constraint for the F_2 folding is given by four different results; the age of the syn-kinematic Rocha Granite, the age of the dacitic dykes crosscutting the Rocha Formation, the age of the white mica of the Laguna de Rocha Shear Zone, and the age of the Santa Teresa Granitic Complex. First, from a regional point of view, the Rocha Granite, syn-kinematic to the neighboring Álferez-Cordillera Shear Zone, indicates that shearing was taking place in the region at ca. 565–560 Ma (Will et al. 2019, this work). Second, the syn-kinematic muscovites of the Laguna de Rocha Shear Zone indicate that by the age of ca. 565 Ma, the shearing system was active and getting cooled beneath the temperature of 450 °C, but the age of the fine-grained white mica fractions indicate that further low-temperature shearing took place up to ca. 535–525 Ma. Third, the age of the dacitic dykes crosscutting the F_2 structures of the Rocha Formation gave an age of 565 Ma, also do not show major signs of deformation. Fourth, the Santa Teresa Granitic complex, with an age of ca. 543 Ma (Basei et al. 2013), intrusive to the Rocha Formation, also crosscut the F_2 structures. Therefore, based on the available ages, we can describe the following deformation pattern for the F_2: (a) folding begins at ca. 570 Ma, (b) progressive strain localization. At the age of ca. 565 Ma, the temperature conditions in the Laguna de Rocha Shear Zone cooled beneath 450 °C and contemporaneously, the already formed F_2 structures were intruded by non-deformed dacitic dykes with a measured age of ca. 565 Ma. Similarly, by this age, the Rocha granite intruded in the neighboring Cordillera Shear Zone, (c) finally, the Santa Teresa Granitic Complex intruded the Rocha Formation, also crosscutting the F_2 structures. Any further deformation was by this time already localized within the Laguna de Rocha Shear Zone, as indicated by the fine white mica fractions. On the African side, the Gariep Belt shows a series of structural similarities that suggest a similar evolution to the one recorded in the Rocha Formation, with a main transpressive event and transpressive re-folding (e.g. Jasper et al. 1992; Hälbich und Alchin 1995; Gray et al. 2008; Brayshaw and Watkeys 2018).

On the other hand, the Paso del Dragón Complex shows a complex stratigraphy, hindering the previously proposed correlations with the Rocha Formation (Peel et al. 2018). The complex is composed of two different tectonically intercalated units, probably with dissimilar origins, namely the metamafic and paraderived rocks, contrary to the Rocha Formation. While metamafic rocks show a roughly Tonian to Cryogenian crystallization age (704 ± 58 Ma, Chavez Ramos et al. 2020) and metamorphism at 628–625 Ma (Will et al. 2019), the paraderived sequence shows a maximum deposition age at about 660 Ma and an Ediacaran metamorphism at ca. 570 Ma. Both units, mafic and metasedimentary are probably tectonically intermixed since the Ediacaran, as

shown by the relationships with the intrusive bodies, for example the Três Figueiras Granite, with an age of 585 Ma.

In spite of the proposed relationships between the Rocha Formation and the Paso del Dragón Complex (Peel et al. 2018; Vieira et al. 2019), the latter records a spectrum with large Meso- and Paleoproterozoic populations, more comparable with spectra of the paraderived rocks of the Cerro Olivo Complex (Fig. 14). Evidence thus suggests that the Paso del Dragon Complex is not directly related to the Rocha Formation. Further studies of this complex will allow to discard or confirm a correlation between both.

Correlations and general evolution

The Punta del Este Terrane is possibly one of the most controversial tectonostratigraphic blocks within the basement configuration of the Dom Feliciano Belt. It has been alternatively correlated with rocks of the Coastal Terrane in the Kaoko Belt (e.g. Oyhantçabal et al. 2009; Konopasek et al. 2017) and the western Kalahari Craton (e.g. Blanco et al. 2011; Frimmel et al. 2011, 2013), which implies contrasting origins related to the Congo or Kalahari Craton, respectively.

Tonian orthogneisses of the Punta del Este Terrane basement show clearly subchondritic Lu–Hf compositions ($\varepsilon Hf_{(t)}$ from −12 to −4), suggesting a significant recycling of paragneisses dominated by Meso- to Paleoproterozoic detrital zircons with mainly suprachondritic compositions (Fig. 12). Though late Mesoproterozoic and Tonian detrital zircons are abundant in the Rocha Formation, they yield contrasting suprachondritic compositions, discarding a possible source in the basement of the Punta del Este Terrane.

The Lu–Hf zircon isotopic composition of ortho- and paragneisses of the Punta del Este Terrane basement are clearly different from that of coeval detrital zircons in the Saldania and Gariep Belts in the western Kalahari Craton (Frimmel et al. 2013; Hofmann et al. 2014; Oriolo and Becker, 2018), which is, however, comparable with detrital zircons of the Rocha Formation (Fig. 19). These similarities further reinforce correlations of the Rocha Formation with coeval sequences of the Gariep Belt, particularly the Oranjemund Group of the Marmora Terrane, as previously suggested (e.g. Basei et al. 2005; Blanco et al. 2011; Abre et al. 2020), but seem to rule out a derivation from the Punta del Este Terrane basement. On the other hand, the latter seems to have an affinity with the Coastal Terrane of the Kaoko Belt, as already indicated by Oyhantçabal et al. (2009) and Konopasek et al. (2017), among others. This correlation is well-documented in the similar magmatic and metamorphic ages (Fig. 15), as well as in the detrital zircon spectra of the paraderived rocks (Fig. 16) and the geochemistry of the orthogneisses.

In this context, previous proposals indicating a Kalahari affinity for the Punta del Este Terrane do not seem to be valid, since the Rocha Formation seems to be the only sequence correlatable with that crustal block. The lack of Ediacaran zircons in the latter suggests that derivation from the Dom Feliciano Belt granitoids, which are widespread at ca. 620–570 Ma in the Punta del Este Terrane, is unlikely. Therefore, it could be inferred that deposition of the Rocha Formation took place together with comparable equivalents of the Gariep Belt, closer to the Kalahari Craton, where Ediacaran magmatism at ca. 630–570 Ma is absent. Consequently, the Rocha Formation seems to be allochthonous to the Dom Feliciano Belt and was possibly accreted to the latter prior to ca. 580 Ma, as suggested by the structural relationships with the Sierra de Aguirre Formation.

The aforementioned model satisfactorily explains all the geological and geochronological data of the Punta del Este Terrane, and reconciles contrasting hypotheses about its African origins (e.g. Frimmel et al. 2011). This implies a "two-stage" evolution of the Dom Feliciano Belt, with an early Ediacaran collision of the Rio de la Plata and Congo cratons, succeeded by the late Ediacaran assembly of the Kalahari Craton to the former (e.g. Rapela et al. 2011; Oriolo et al. 2016). The Rio de la Plata-Congo collision triggered the accretion of Congo/Angola-derived blocks, including the Punta del Este Terrane, to the margin of the Rio de la Plata Craton. Subsequent convergence, possibly starting at ca. 600–590 Ma (Lehmann et al. 2016), finally lead to the juxtaposition of the Kalahari Craton and marginal Gariep sequences, including the Rocha Formation, to the southeastern most Dom Feliciano Belt.

Conclusions

New zircon U–Pb and Lu–Hf data from ortho- and paragneisses of the Cerro Olivo Complex indicate that the basement of the Punta del Este Terrane does not comprise a large Mesoproterozoic crustal block but, instead, is mainly constituted of Early Neoproterozoic metaigneous and metasedimentary rocks. A Tonian retreating-mode accretionary orogen seems to be the most likely tectonic setting for this complex, which reconciles previous models suggesting arc vs. rift magmatism. Isotopic data allow us to discard the Nico Pérez Terrane as an important source for the magmatism or the sediments of the Punta del Este Terrane. Instead, previous correlations with the Coastal Terrane of the Kaoko Belt are confirmed, based on similarities in magmatic and metamorphic ages, as well as in the detrital zircon spectra of paraderived rocks of both blocks.

The deposition age of the Rocha Formation is constrained between the youngest detrital zircon age peak, at ca. 660 Ma, and the beginning of the deposition of the Sierra de Aguirre Formation at ca. 580 Ma, based on

the structural relationship between them. Detrital zircon data of the Rocha Formation also indicate that it was not sourced in the Dom Feliciano Belt, but shares the sources of the Marmora Terrane, further reinforcing previous correlations with the Gariep Belt. It is thus proposed that the Rocha Formation belongs to the former and was only juxtaposed by the late Ediacaran to the South American margin. Deposition of the Sierra de Aguirre Formation at ca. 580 Ma represents the maximum age for the accretion of the Gariep Belt, including the Rocha Formation, to the Punta del Este Terrane.

As a corollary, a two-stage evolution model is considered as the most satisfactory explanation for the tectonometamorphic and sedimentary evolution of the Dom Feliciano Belt, with an early Ediacaran collision of the Rio de la Plata and Congo cratons, succeeded by the late Ediacaran assembly of the Kalahari Craton to the former.

Supplementary Information The online version contains supplementary material available at https://doi.org/10.1007/s00531-022-02230-0.

Acknowledgements Hernan Silva thanks the DAAD for the long-term PhD scholarship (R.N. 91727773). Mathias Hueck thanks the FAPESP for a post-doctoral fellowship (2019/06838-2). Part of the work was funded by the FAPESP thematic project 2015/03737-0, coordinated by Miguel A.S. Basei.

Funding Open Access funding enabled and organized by Projekt DEAL.

Declarations

Conflict of interest The authors state that there is no conflict of interest related to this work.

References

Abre P, Blanco G, Gaucher C, Frei D, Frei R (2020) Provenance of the late ediacaran Rocha Formation, Cuchilla Dionisio Terrane, Uruguay: tectonic implications on the assembly of Gondwana. Precambrian Res 342:105407. https://doi.org/10.1016/j.precamres.2020.105704

Andersen T, Elburg MA, van Niekerk HS, Ueckermann H (2018) Successive sedimentary recycling regimes in southwestern Gondwana: evidence from detrital zircons in Neoproterozoic to Cambrian sedimentary rocks in southern Africa. Earth-Sci Rev 181:43–60. https://doi.org/10.1016/J.earscirev.2018.04.001

Andersen T, Elburg MA, Magwaza BN (2019) Sources of bias in detrital zircon geochronology: discordance, concealed lead loss and common lead correction. Earth-Sci Rev 197:102899. https://doi.org/10.1016/j.earscirev.2019.102899

Arena KR, Hartmann LA, Lana C (2016) Evolution of neoproterozoic ophiolites from the southern Brasiliano Orogen revealed by zircon U–Pb–Hf isotopes and geochemistry. Precambrian Res 285:299–314. https://doi.org/10.1016/j.precamres.2016.09.014

Babinski M, Chemale F Jr, Hartmann LA, van Schmus WR, da Silva LC (1996) Juvenile accretion at 750–700 Ma in southern Brazil. Geology 24:439–442. https://doi.org/10.1130/0091-7613(1996)024%3c0439:JAAMIS%3e2.3.CO;2

Ballivián Justiniano CA, Basei MAS, Sato AM, González PD, Benítez ME, Lanfranchini ME (2020) The Neoproterozoic basement of the Sauce Chico Inlier (Ventania System): Geochemistry and U–Pb geochronology of igneous rocks with African lineage in central-eastern Argentina. J S Am Earth Sci 98:10–39. https://doi.org/10.1016/j.jsames.2019.102391

Basei MAS, Frimmel HE, Nutman AP, Preciozzi F, Jacob J (2005) A connection between the Neoproterozoic Dom Feliciano (Brazil/Uruguay) and Gariep (Namibia/South Africa) orogenic belts—evidence from a reconnaissance provenance study. Precambrian Res 139:195–221. https://doi.org/10.1016/j.precamres.2005.06.005

Basei MAS, Brito Neves BB, Siga O Jr, Babinski M, Pimentel MM, Hollanda MHB, Nutman A, Cordani UG (2010) Contributions of SHRIMP U–Pb zircon geochronology to unravelling the evolution of Brazilian Neoproterozoic fold belts. Precambrian Res 183(112):144. https://doi.org/10.1016/j.precamres.2010.07.015

Basei MAS, Drukas CO, Nutman AP, Wemmer K, Dunyi L, Santos PR, Passarelli CR, Campos Neto MC, Siga O Jr, Osako L (2011) The Itajaí foreland basin: a tectono-sedimentary record of the Ediacaran period. Southern Brazil Int J Earth Sci 100(2–3):543–569. https://doi.org/10.1007/s00531-010-0604-4

Basei MAS, Siga O Jr, Masquelin H, Harara OM, Reis Neto JM, Preciozzi, F (2000) The Dom Feliciano Belt of Brazil and Uruguay and its foreland domain. In: Cordani U, Milani EJ, Thomas FA, Campos AD (eds) Tectonic Evolution of South America. 31st Int Geol Congress, Rio de Janiero, pp 311–334

Basei MAS, Grasso C, Vlach SRF, Nutman AP, Siga Jr O, Osako LS (2008b) A-type rift-related granite and the Lower Cryogenian age for the beginning of the Brusque Belt basin. In: VI S Am Symp on Isotope Geol, San Carlos de Bariloche, Argentina

Basei MAS, Peel E, Muzio R (2013) Geocronologia U–Pb LA–ICP–MS en circones del Complejo Granitico Santa Teresa, Terreno Punta del Este. In: VII Congreso Uruguayo de Geologia, Programa, pp 30–31

Basei MAS, Frimmel H, Campos Neto MC, Araújo CA, Castro NA, Passarelli C R (2018) The Tectonic History of the Southern Adamastor Ocean Based on a Correlation of the Kaoko and Dom Feliciano Belts. In: Siegesmund S, Oyhantçabal P, Basei MAS, Oriolo S (eds) Geology of Southwest Gondwana. Regional Geology Reviews. Springer, Cham. https://doi.org/10.1007/978-3-319-68920-3_3

Beloni MS, Porcher CC, Koester E, Ramos C, Lana C, Wegne AC (2016) Caracterização U/Pb de zircão detrítico e geoquímica isotópica (Sm/Nd) em rocha-total dos xistos e quartzitos de Arroio Grande–RS. XLVIII Congresso Brasileiro de Geologia, Porto Alegre, Brasil

Bettucci LS, Burgueño AM (1993) Análisis Sedimentológico y Faciológico de la Formación Rocha (ex-Grupo Rocha). Rev Brasil

Geociên 23(3):323–329. https://doi.org/10.25249/0375-7536.1993233323329
Bitencourt MF, Nardi LVS (2000) Tectonic setting and sources of magmatism related to the Southern Brazilian shear Belt. Rev Brasil Geociên 30:186–189. https://doi.org/10.25249/0375-7536.2000301186189
Blanco G, Germs GJB, Rajesh HM, Chemale F Jr, Dussin IA, Justino D (2011) Provenance and paleogeography of the Nama Group (Ediacaran to early Palaeozoic, Namibia): Petrography, geochemistry and U–Pb detrital zircon geochronology. Precambrian Res 187:15–32. https://doi.org/10.1016/j.precamres.2011.02.002
Blanco G, Abre P, Cabrera J, Gaucher C (2014) Formación Rocha. In: Bossi J, Gaucher C (eds) Geología del Uruguay—Tomo 1: Predevónico, Montevideo, pp 401–408
Blichert-Toft J, Albarède F (1997) The Lu–Hf geochemistry of chondrites and the evolution of the mantle-crust system. Earth Planet Sci Lett 148:243–258
Bossi J, Navarro R (1991) Geologia del Uruguay, Universidad de la República, Montevideo, vol 1, p 453
Bossi J, Gaucher C (2004) The Cuchilla Dionisio Terrane, Uruguay: an allochthonous block accreted in the cambrian to SW-Gondwana. Gondwana Res 7(3):661–674. https://doi.org/10.1016/S1342-937X(05)71054-6
Brayshaw MM, Watkeys MK (2018) Structural evolution and architecture of the outer margin of the Gariep Belt at Rosh Pinah, southern Namibia. S Afr J Geol 121(2):171–190. https://doi.org/10.25131/sajg.121.0011
Brito Neves BB, Fuck RA (2014) The basement of South American platform: half Gondwana half Laurentia. Precambr Res 244:75–86. https://doi.org/10.1016/j.precamres.2013.09.020
Brown M (2013) Granite: from genesis to emplacement. GSA Bull 125(7/8):1079–1113. https://doi.org/10.1130/B30877.1
Burkhard M (1993) Calcite twins, their geometry, appearance and significance as stress-strain markers and indicators of tectonic regime: a review. J Struct Geol 15(3–5):351–368. https://doi.org/10.1016/0191-8141(93)90132-T
Campal N, Gancio F (1993) Asociacion volcanitas piroclastitas de los Cerros Aguirre (Dpto. de Rocha): una nueva formacion y su implicancia en la evolucion del Ciclo Brasiliano en el Uruguay. In: I Symp Int del Neoproterozoico—Cambrico de la Cuenca del Plata, Resumenes Extensos 2. La Paloma, Uruguay, no 44
Campal N, Schipilov A (2005) La Formacion Cerros de Aguirre: Evidencias de Magmatismo Vendiano en el Uruguay. Lat Am J Sedimentol Basin Anal 12:161–174
Cawood PA, Hawkesworth CJ, Dhuime B (2012) Detrital zircon record and tectonic setting. Geology 40(10):875–878. https://doi.org/10.1130/G32945.1
Caxito FA, Heilbron M, Valeriano CM, Bruno H, Pedrosa-Soares A, Alkmim FF, Basei MAS (2021) Integration of elemental and isotope data supports a neoproterozoic adamastor ocean realm. Geochem Persp Let 17:6–10. https://doi.org/10.7185/geochemlet.2106
Caxito FA, Hartmann LA, Heilbron M, Pedrosa-Soares AC, Bruno H, Basei MAS, Chemale F (2022) Multi-proxy evidence for subduction of the Neoproterozoic Adamastor Ocean and Wilson cycle tectonics in the South Atlantic Brasiliano Orogenic System of Western Gondwana. Precambrian Res 376:106678. https://doi.org/10.1016/j.precamres.2022.106678
Chappell BW, White AJR (1992) I- and S-type granites in the lachlan fold belt. Trans R Soc Edinb Earth Sci 83(1–2):1–26. https://doi.org/10.1130/SPE272-p1
Chappell BW, Bryant CJ, Wyborn D (2012) Peraluminous I-type granites. 7th Hutton Symp. Lithos 153:142–153. https://doi.org/10.1016/j.lithos.2012.07.008
Christiansen RO, Justiniano CAB, Oriolo S, Gianni GM, García HP, Martinez MP, Kostadinoff J (2021) Crustal architecture and tectonic evolution of the southernmost Río de la Plata Craton and its Neoproterozoic-Paleozoic sedimentary cover: insights from 3D litho-constrained stochastic inversion models. Precambrian Res 362:106307. https://doi.org/10.1016/j.precamres.2021.106307
Colliston WP, Cornell WP, Schoch AE (2015) Geochronological constraints on the Hartbees River Thrust and Augrabies Nappe: new insights into the assembly of the Mesoproterozoic Namaqua-Natal Province of Southern Africa. Precambrian Res 265:150–165. https://doi.org/10.1016/j.precamres.2015.03.008
Cordani UG, Amaral G, Kawashita K (1973) The precambrian evolution of South America. Geol Rundsch 62(2):309–317
Cordani UG, D'Agrella-Filho MS, Brito-Neves BB, Trindade RIF (2003) Tearing up Rodinia: the Neoproterozoic palaeogeography of South American cratonic fragments. Terra Nova 15:350–359. https://doi.org/10.1046/j.1365-3121.2003.00506.x
Cornell DH, van Schijndel V, Simonsen SL, Frei D (2015) Geochronology of Mesoproterozoic hybrid intrusions in the Konkiep Terrane, Namibia, from passive to active continental margin in the Namaqua-Natal Wilson Cycle. Precambrian Res 265:166–188. https://doi.org/10.1016/j.precamres.2014.11.028
Coutts DS, Matthews WA, Hubbard SM (2019) Assessment of widely used methods to derive depositional ages from detrital zircon populations. Geosci Front 10764:1421–1435. https://doi.org/10.1016/j.gsf.2018.11.002
Cruz RF (2017) O Terreno Jaguarão: Caracterização de Novo Domínio Geológico no Sudeste do Rio Grande do Sul. In: X Int Symp tectonics (CD-ROM)
De Toni GB, Bitencourt MF, Nardi LVS, Florisbal LM, Almeida BS, Geraldes M (2020) Dom Feliciano Belt orogenic cycle tracked by its pre-collisional magmatism: the Tonian (ca. 800 Ma) Porto Belo Complex and its correlations in southern Brazil and Uruguay. Precambrian Res 342:105702. https://doi.org/10.1016/j.precamres.2020.105702
De Toni GB, Bitencourt MF, Konopásek J, Battisti MA, da Costa EO, Savian JF (2021) Autochthonous origin of the Encruzilhada Block, Dom Feliciano Belt, southern Brazil, based on aerogeophysics, image analysis and PT-paths. J Geodyn 144:101825. https://doi.org/10.1016/j.jog.2021.101825
Foster DA, Goscombe BD, Newstead B, Mapani B, Mueller PA, Gregory LC, Muvangua E (2014) U–Pb age and Lu–Hf isotopic data of detrital zircons from the Neoproterozoic Damara Sequence: Implications for Congo and Kalahari before Gondwana. Gondwana Res 28:179–190. https://doi.org/10.1016/j.gr.2014.04.011
Frimmel HE (2010) On the reliability of stable carbon isotopes for Neoproterozoic chemostratigraphic correlation. Precambrian Res 182(4):0–253. https://doi.org/10.1016/j.precamres.2010.01.003
Frimmel HE (2018) The Gariep Belt. In: Siegesmund S, Basei MAS, Oyhantçabal P, Oriolo S (eds) Geology of Southwest Gondwana. Regional Geology Reviews. Springer, Cham. https://doi.org/10.1007/978-3-319-68920-3_13
Frimmel HE, Fölling PG (2003) Late Vendian closure of the Adamastor Ocean: timing of tectonic inversion and syn-orogenic sedimentation in the Gariep Basin. Gondwana Res 7(3):685–699. https://doi.org/10.1016/S1342-937X(05)71056-X
Frimmel HE, Frank W (1998) Neoproterozoic tectono-thermal evolution of the Gariep Belt and its basement, Namibia and South Africa. Precambrian Res 90(1–2):1–28. https://doi.org/10.1016/S0301-9268(98)00029-1
Frimmel HE, Fölling PG, Eriksson PG (2002) Neoproterozoic tectonic and climatic evolution recorded in the Gariep Belt, Namibia and South Africa. Basin Res 14:55–67. https://doi.org/10.1046/j.1365-2117.2002.00166.x
Frimmel HE, Basei MAS, Gaucher C (2011) Neoproterozoic geodynamic evolution of SW-Gondwana: a southern African

perspective. Int J Earth Sci 100(2):323–354. https://doi.org/10.1007/s00531-010-0571-9
Frimmel HE, Basei MAS, Correa VX, Mbangula N (2013) A new lithostratigraphic subdivision and geodynamic model for the Pan-African western Saldania Belt, South Africa. Precambrian Res 231:218–235. https://doi.org/10.1016/j.precamres.2013.03.014
Frost CD, Frost BR (2011) On ferroan (A-type) granitoids: their compositional variability and modes of origin. J Petrol 52(1):39–53. https://doi.org/10.1093/petrology/egq070
Gallardo Silveira P, Peel E, Fort S (2016) Caracterizacion geoquímica del complejo granítico Polanco, (Edicarico-Cambrico). VIII Congreso Uruguayo de Geologia, Montevideo, actas, p 245
Gaucher C, Frimmel HE, Germs GJB (2009) Tectonic events and palaeogeographic evolution of Southwestern Gondwana in the Neoproterozoic and Cambrian. In: Gaucher C, Sial AN, Halverson GP, Frimmel HE (eds): Neoproterozoic-Cambrian tectonics, global change and evolution: a focus on southwestern Gondwana. Developments in Precambrian Geology 16:295–316. https://doi.org/10.1016/S0166-2635(09)01621-1
Gaucher C, Frei R, Chemale F Jr, Frei D, Bossi J, Martínez G, Chiglino L, Cernuschi F (2011) Mesoproterozoic evolution of the Río de la Plata Craton in Uruguay: at the heart of Rodinia? Int J Earth Sci 100(2):273–288. https://doi.org/10.1007/s00531-010-0562-x
Gaucher C, Bossi J, Frei R, Remus M, Piñeyro D (2014) Terreno Cuchilla Dionisio: bloque septentrional. In: Bossi J, Gaucher C (eds.) Geología del Uruguay. Tomo 1: Predevónico. Polo, Montevideo, pp 377–400
Goscombe B, Gray DR (2007) The Coastal Terrane of the Kaoko Belt, Namibia: outboard arc-terrane and tectonic significance. Precambr Res 155(1–2):139–158. https://doi.org/10.1016/j.precamres.2007.01.008
Goscombe B, Gray D, Armstrong R, Foster DA, Vogl J (2005) Event geochronology of the Pan-African Kaoko Belt, Namibia. Precambrian Res 140(3–4):103.e1-103.e41. https://doi.org/10.1016/j.precamres.2005.07.003
Goscombe B, Foster DA, Gray D, Wade B, Marsellos A, Titus J (2017a) Deformation correlations, stress field switches and evolution of an orogenic intersection: the Pan-African Kaoko-Damara orogenic junction, Namibia. Geosci Front 8(6):1187–1232. https://doi.org/10.1016/j.gsf.2017.05.001
Goscombe B, Foster DA, Gray D, Wade B (2017b) Metamorphic response and crustal architecture in a classic collisional orogen: the Damara Belt, Namibia. Gondwana Res 52:80–124. https://doi.org/10.1016/j.gr.2017.07.006
Goscombe B, Gray DR (2008) Structure and strain variation at mid-crustal levels in a transpressional orogen: a review of Kaoko Belt structure and the character of West Gondwana amalgamation and dispersal. Gondwana Res 13(1):45–85. https://doi.org/10.1016/j.gr.2007.07.002
Goscombe B, Foster DA, Gray D, Wade B (2018) The evolution of the Damara orogenic system: a record of west Gondwana assembly and crustal response. In: Siegesmund S, Oyhantçabal P, Basei MAS, Oriolo S (eds) Geology of Southwest Gondwana. Regional Geology Reviews. Springer, Cham. https://doi.org/10.1007/978-3-319-68920-3_12
Gray DR, Foster DA, Meert JG, Goscombe BD, Armstrong R, Trouw RAJ, Passchier CW (2008) A Damara orogen perspective on the assembly of southwestern Gondwana. Geol Soc Spec Publ 294(1):257–278. https://doi.org/10.1144/SP294.14
Griffin WL, Wang X, Jackson SE, Pearson NJ, O'Reilly S, Xu X, Zhou X (2002) Zircon chemistry and magma mixing, SE China: in-situ analysis of Hf isotopes, Tonglu and Pingtan igneous complexes. Lithos 61(3–4):237–269. https://doi.org/10.1016/S0024-4937(02)00082-8
Gross AOMS, Porcher CC, Fernandes LAD, Koester E (2006) Neoproterozoic low-pressure/high-temperature colisional metamorphic evolution in the Varzea do Capivarita Metamorphic Suite, SE Brazil: thermobarometric and Sm/Nd evidence. Precambr Res 147(1):41–64. https://doi.org/10.1016/j.precamres.2006.02.001
Gross AOMS, Droop GTR, Porcher CC, Fernandes LAD (2009) Petrology and thermobarometry of mafic granulites and migmatites from the Chafalote Metamorphic Suite: new insights into the Neoproterozoic P–T evolution of the Uruguayan-Sul Rio Grandes shield. Precambrian Res 170(3–4):157–174. https://doi.org/10.1016/j.precamres.2009.01.011
Gubert ML, Philipp RP, Basei MAS (2016) The Bossoroca Complex, São Gabriel Terrane, Dom Feliciano Belt, southermost Brazil: U–Pb geochronology and tectonic implications for the Neoproterozoic São Gabriel Arc. J S Am Earth Sci 70:1–17. https://doi.org/10.1016/j.jsames.2016.04.006
Hälbich IW, Alchin DJ (1995) The Gariep belt: stratigraphic-structural evidence for obliquely transformed grabens and back-folded thrust stacks in a combined thick-skin thin-skin structural setting. J Afr Earth Sci 21(1):9–33. https://doi.org/10.1016/0899-5362(95)00080-D
Hartmann LA, Campal N, Santos JOS, McNaughton NJ, Bossi J, Schipilov A, Lafon JM (2001) Archean crust in the Rio de la Plata Craton, Uruguay—SHRIMP U–Pb zircon reconnaissance geochronology. J S Am Earth Sci 14(6):557–570. https://doi.org/10.1016/S0895-9811(01)00055-4
Hartmann LA, Santos JOS, Bossi J, Campal N, Schipilov A, McNaughton NJ (2002) Zircon and titanite U–Pb SHRIMP geochronology of neoproterozoic felsic magmatism on the eastern border of the Río de la Plata Craton, Uruguay. J S Am Earth Sci 15(2):229–236. https://doi.org/10.1016/S0895-9811(02)00030-5
Heilbron M, Valeriano CM, Tassinari CCG, Almeida J, Tupinambá M, Siga Jr O, Trouw R (2008) Correlation of Neoproterozoic terranes between the Ribeira Belt, SE Brazil and its African counterpart: comparative tectonic evolution and open questions. In: Pankhurst RJ, Trouw RAJ, Brito Neves BB and De Wit MJ (eds) West Gondwana: Pre-Cenozoic Correlations across the South Atlantic Region, Geol Soc London Spec Publ 294(1):211–237. https://doi.org/10.1144/SP294.12
Hofmann M, Linnemann U, Hoffmann KH, Gerdes A, Eckelmann K, Gärtner A (2014) The Namuskluft and Dreigratberg sections in southern Namibia (Kalahari Craton, Gariep Belt): a geological history of Neoproterozoic rifting and recycling of cratonic crust during the dispersal of Rodinia. Int J Earth Sci 103(5):1187–1202. https://doi.org/10.1007/s00531-013-0949-6
Hofmann M, Linnemann U, Hoffmann KH, Germs G, Gerdes A, Marko, L, Eckelman K, Gärtner A, Krause R (2015). The four Neoproterozoic glaciations of southern Namibia and their detrital zircon record: the fingerprints of four crustal growth events during two supercontinent cycles. Precambrian Res 259:176–188. https://doi.org/10.1016/j.precamres.2014.07.021
Hueck M, Basei MAS, de Castro NA (2016) Origin and evolution of the granitic intrusions in the Brusque Group of the Dom Feliciano Belt, south Brazil: petrostructural analysis and whole-rock/isotope geochemistry. J S Am Earth Sci 69:131–151. https://doi.org/10.1016/j.jsames.2016.04.004
Hueck M, Oriolo S, Dunkl I, Wemmer K, Oyhantçabal P, Schanofski M, Basei MAS, Siegesmund S (2017) Phanerozoic low-temperature evolution of the uruguayan shield along the South American passive margin. J Geol Soc 174(4):609–626. https://doi.org/10.1144/jgs2016-101
Hueck M, Basei MAS, Wemmer K, Oriolo S, Heidelbach F, Siegesmund S (2019) Evolution of the Major Gercino Shear Zone in the Dom Feliciano Belt, South Brazil, and implications for the assembly of southwestern Gondwana. Int J Earth Sci 108(2):403–425. https://doi.org/10.1007/s00531-018-1660-4
Hueck M, Wemmer K, Basei MAS, Philipp RP, Oriolo S, Heidelbach F, Oyhantçabal P, Siegesmund S (2020a) Dating recurrent shear

zone activity and the transition from ductile to brittle deformation: white mica geochronology applied to the Neoproterozoic Dom Feliciano Belt in South Brazil. J Struct Geol. https://doi.org/10.1016/j.jsg.2020.104199

Hueck M, Oriolo S, Basei MAS, Oyhantçabal P, Heller BM, Wemmer K, Siegesmund S (2022) Archean to early Neoproterozoic crustal growth of the southern South American Platform and its wide-reaching "African" origins. Precambrian Res 369:106532. https://doi.org/10.1016/j.precamres.2021.106532

Hueck M, Oyhantçabal P, Philipp RP, Basei MAS, Siegesmund S (2018) The Dom Feliciano Belt in Southern Brazil and Uruguay. In: Siegesmund S, Basei MAS, Oyhantçabal P, Oriolo S (eds) Geology of Southwest Gondwana. Regional Geology Reviews. Springer, Cham. https://doi.org/10.1007/978-3-319-68920-3_11

Hueck M, Basei MAS, Castro NA (2020b) Tracking the sources and the evolution of the late Neoproterozoic granitic intrusions in the Brusque Group, Dom Feliciano Belt, South Brazil: LA–ICP–MS and SHRIMP geochronology coupled to Hf isotopic analysis. Precambrian Res. https://doi.org/10.1016/j.precamres.2019.105566

Janikian L, Almeida RP, Fragoso-Cesar ARS, Martins VTS, Dantas EL, Tohver E, McReath I, D'Agrella-Filho MS (2012) Ages (U–Pb SHRIMP and LA ICPMS) and stratigraphic evolution of the Neoproterozoic volcano-sedimentary successions from the extensional Camaquã Basin, Southern Brazil. Gondwana Res 21:466–482. https://doi.org/10.1016/j.gr.2011.04.010

Janikian L (2004) Sequências deposicionais e evolução paleoambiental do Grupo Bom Jardim e da Formação Acampamento Velho, Supergrupo Camaquã. Rio Grande do Sul. PhD thesis, São Paulo University, p 189

Jasper MJU, Stanistreet JG, Charlesworth EG (1992) Report: Preliminary results of a study of the structural and sedimentological evolution of the late Proterozoidearly Palaeozoic Gariep Belt, southern Namibia. Commun Geol Surv Namibia 8(1992/93):105–126

Kelemen PB, Shim N, Dunn T (1993) Relative depletion of niobium in some arc magmas and the continental crust: partitioning of K, Nb, La and Ce during melt/rock reaction in the upper mantle. Earth Planet Sci Lett 120:111–134. https://doi.org/10.1016/0012-821X(93)90234-Z

Klein FG, Koester E, Vieira DT, Porcher CC, Ramos RC, Philipp RP (2018) Geologia do Granito Tres Figueiras: magmatismo peraluminoso de 585 Ma no sudeste do Cinturao Dom Feliciano. Pesqui em Geocienc 45(2):1–27. https://doi.org/10.22456/1807-9806.88646

Koester E, Porcher CC, Pimentel MM, Fernandes LAD, Vignol-Lelarge ML, Oliveira LD, Ramos RC (2016) Further evidence of 777 Ma subduction-related continental arc magmatism in Eastern Dom Feliciano Belt, southern Brazil: the Chácara das Pedras Orthogneiss. J S Am Earth Sci 68:155–166. https://doi.org/10.1016/j.jsames.2015.12.006

Konopásek J, Kröner S, Kitt SL, Passchier CW, Kröner A (2005) Oblique collision and evolution of large-scale transcurrent shear zones in the Kaoko belt, NW Namibia. Precambrian Res 136:139–157. https://doi.org/10.1016/j.precamres.2004.10.005

Konopásek J, Kosler J, Sláma J, Janousek V (2014) Timing and sources of pre-collisional Neoproterozoic sedimentation along the SW margin of the Congo Craton (Kaoko Belt, NW Namibia). Gondwana Res 26:386–401. https://doi.org/10.1016/j.gr.2013.06.021

Konopásek J, Sláma J, Kosler J (2016) Linking the basement geology along the Africa-South America coasts in the South Atlantic. Precambrian Res 280:221–230. https://doi.org/10.1016/j.precamres.2016.05.011

Konopásek J, Janousek V, Oyhantçabal P, Sláma J, Ulrich S (2017) Did the circum-Rodinia subduction trigger the Neoproterozoic rifting along the Congo-Kalahari Craton margin? Int J Earth Sci 107(5):1859–1894. https://doi.org/10.1007/s00531-017-1576-4

Konopásek J, Cavalcante C, Fossen H, Janousek V (2020) Adamastor—An ocean that never existed? Earth-Sci Rev 205:103201. https://doi.org/10.1016/j.earscirev.2020.103201

Konopásek J, Kosler J, Tajcmanova L, Ulrich S, Kitt S (2008) Neoproterozoic igneous complex emplaced along major tectonic boundary in the Kaoko Belt (NW Namibia): Ion probe and LAICP–MS dating of magmatic and metamorphic zircons. J Geol Soc Lond 165(1):153–165. https://doi.org/10.1144/0016-76492006-192

Kröner A (1984) Late Precambrian plate tectonics and orogeny: a need to redefine the term Pan-African. In: Klerkx J, Michot J (eds) Geologie Africaine. African Geology, Tervuren, pp 23–28

Kröner A, Cordani U (2003) African, southern Indian and South American cratons were not part of the Rodinia supercontinent: evidence from field relationships and geochronology. Tectonophysics 375(1–4):0–352. https://doi.org/10.1016/s0040-1951(03)00344-5

Lara P, Oyhantçabal P, Belousova E (2020) Two distinct crustal sources for Late Neoproterozoic granitic magmatism across the Sierra Ballena Shear Zone, Dom Feliciano Belt, Uruguay: whole-rock geochemistry, zircon geochronology and Sr–Nd–Hf isotope evidence. Precambrian Res 341:105625. https://doi.org/10.1016/j.precamres.2020.105625

Lara P, Oyhantçabal P, Elena B, Hueck M (2021) Source diversity of Late Neoproterozoic granitoid magmatism across an orogen-scale lineament in southern Brazil and Uruguay: whole-rock geochemistry, zircon geochronology and Sr–Nd–Hf isotope evidence. J S Am Earth Sci 112(3–4):103597. https://doi.org/10.1016/j.jsames.2021.103597

Lara P, Oyhantcabal P, Dadd K (2013) Late Neoproterozoic high-Barium-Strontium granitic magmatism of the Uruguayan Precambrian Shield. In: Sociedad Uruguaya de Geología (ed) VII Congreso Uruguayo de Geologia, CD ROM, Montevideo, Uruguay

Lara P, Oyhantçabal P, Dadd K (2016) Cortez Blanco Pluton: a post-collisional, Late Neoproterozoic, shoshonitic granite from the south-eastern section of the Dom Feliciano Belt, Uruguay. In: Sociedad Uruguaya de Geología (ed) VIII Congreso Uruguayo de Geología, CD-ROM. Montevideo, Uruguay

Lehmann J, Saalmann K, Naydenov K, Milani L, Belyanin G, Zwingmann H, Chalesworth EG, Kinnaird JA (2016) Structural and geochronological constraints on the Pan-African tectonic evolution of the northern Damara Belt, Namibia. Tectonics 35(1):103–135. https://doi.org/10.1002/2015TC003899

Leite JAD, Hartmann LA, McNaughton NJ, Chemale F Jr (1998) SHRIMP U/Pb zircon geochronology of Neoproterozoic juvenile and crustal-reworked terranes in southernmost Brazil. Int Geol Rev 40:688–705. https://doi.org/10.1080/00206819809465232

Lenz C, Fernandes LAD, McNaughton NJ, Porcher CC, Masquelin H (2011) U-Pb SHRIMP ages for the Cerro Bori Orthogneisses, Dom Feliciano Belt in Uruguay: Evidences of a ~800 Ma magmatic and ~650 Ma metamorphic event. Precambrian Res 185(3–4):149–163. https://doi.org/10.1016/j.precamres.2011.01.007

Lenz C, Porcher CC, Fernandes LAD, Masquelin H, Koester E, Conceiçao RV (2012) Geochemistry of the Neoproterozoic (800–767 Ma) Cerro Bori orthogneisses, Dom Feliciano belt in Uruguay: tectonic evolution of an ancient continental arc. Mineral Petrol 107(5):785–806. https://doi.org/10.1007/s00710-012-0244-4

Lenz C, Fernandes LAD, Koester E, Porcher CC (2014) Geoquímica e idades U–Pb SHRIMP do magmatismo máfico sin a pós colisional registrado nos ortognaisses do Complexo Cerro Olivo. Uruguai Cad Geociênc 11(1–2):49–60

Lenz C (2010) Evolucão tectônica Précambriana dos ortogneisses do Complexo Cerro Olivo—Domínio Leste do Cinturão Dom

Feliciano no Uruguai. Unpublished thesis. Universidade Federal do Rio Grande do Sul, p 150
Ludwig KR (2008) Isoplot/Ex 4.15. A Geochronological Toolkit for Microsoft Excel. Berkeley Geochronological Center, Berkely, Spec publ 4, p 76
Machado N, Koppe JC, Hartmann LA (1990) A late proterozoic U–Pb age for the Bossoroca Belt, Rio Grande do Sul. Brazil J S Am Earth Sci 3(1–2):87–90. https://doi.org/10.1016/0895-9811(90)90021-R
Mallmann G, Chemale F, Ávila JN, Kawashita K, Armstrong RA (2007) Isotope geochemistry and geochronology of the Nico Pérez Terrane, Rio de la Plata Craton, Uruguay. Gondwana Res 12(4):489–508. https://doi.org/10.1016/j.gr.2007.01.002
Martil MMD, Bitencourt MF, Nardi LVS, Koester E, Pimentel MM (2017) Pre-collisional, Neoproterozoic (ca. 790 Ma) continental arc magmatism in southern Mantiqueira Province, Brazil: geochemicalal and isotopic constraints from the Várzea do Capivarita Complex. Lithos 274–275:39–52. https://doi.org/10.1016/j.lithos.2016.11.011
Martil MMD, Bitencourt MF, Nardi LVS (2011) Caracterização estrutural e petrológica do magmatismo pré-colisional do Escudo Sul-rio-grandense: os ortognaisses do Complexo Metamórfico Várzea do Capivarita. Pesqui Geociênc 38(2):181–201. https://doi.org/10.22456/1807-9806.26383
Martil MMD (2016) O magmatismo de Arco Continental pré-colisional (790 Ma) e a reconstituição espaço-temporal do regime transpressivo (650 Ma) no Complexo Várzea do Capivarita, Sul da Província Mantiqueira. PhD thesis. Instituto de Geociências, Universidade Federal do Rio Grande do Sul. UFRGS. http://www.lume.ufrgs.br/handle/10183/149194
Masquelin H, Tabó F (1990) Memoria explicativa de la Hoja Chafalote, Carta Geologica del Uruguay, DINAMIGE–UdelaR. Montevideo, Scale 1(100):000
Masquelin H, Nessi A, Paris A (2006) Rocas metapeliticas de la Suite Metamorfica Chafalote SE del Escudo Uruguayo. Rev Soc Uruguaya Geol 12:57–72
Masquelin H, Fernandes LAD, Lenz C, Porcher CC, McNaughton NJ (2012) The Cerro Olivo Complex: a pre-collisional Neoproterozoic magmatic arc in Eastern Uruguay. Int Geol Rev 54(10):1161–1183. https://doi.org/10.1080/00206814.2011.626597
Masquelin H, Lara HS, Sánchez-Bettucci L, Demarco PN, Pascual S, Muzio R, Peel E, Scaglia F (2017) Lithologies, structure and basement-cover relationships in the schist belt of the Dom Feliciano Belt in Uruguay. Braz J Geol 47(1):21–42. https://doi.org/10.1590/23174889201720160119
Masquelin H, Aïfa T, Scaglia F, Basei MAS (2021) The Archean Pavas Block in Uruguay: extension and tectonic evolution based on LA–ICP–MS U–Pb ages and airborne geophysics. J S Am Earth Sci 110:103364. https://doi.org/10.1016/j.jsames.2021.103364
Masquelin H, Silva AOM, Porcher CC, Fernandes LAD, Morales E (2001) Geología y geotermobarometría de la Suite Metamórfica Chafalote, basamento prebrasiliano, sureste del Uruguay. In: Actas do XI Congresso Latino Americano de Geologia, Montevideo
Masquelin H, Morales E, Piñeiro G (2002) Geología de las rocas calcosilicatadas de la Suite Parametamórfica Chafalote, Sureste del Uruguay. In: 15. Congreso Argentino de Geología. Conference proceedings, El Calafate, pp 172–177
Masquelin H, Fernandes LAD, Lenz C, McNaughton NJ, Porcher CC, Koester E, Scaglia F (2010) Texturas y edades U–Pb SHRIMP en circones del Complejo Cerro Olivo: Magmatismo neoproterozoico y herencia mesoproterozoica en el sureste de Uruguay. VII South American Symposium on Isotope Geology, Brasilia, pp 89–92
Masquelin H (1993) Análisis geométrico y cinemático de las Supracrustales de Rocha, Uruguay, In: Simposio Internacional sobre Neoproterozoico—Cámbrico de la Cuenca del Plata, La Paloma (I) 21
Masquelin H (2002) Evolução estrutural e metamórfica do Complexo Gnáissico "Cerro Olivo", Sudeste do Uruguai. Tese de Doutorado (PhD), UFRGS, Porto Alegre
Masquelin H (2005) El Escudo Uruguayo. In: Ubilla M, Veroslavsky G (eds) Cuencas Sedimentarias de Uruguay, geologia, paleontologia y recursos minerales: Paleozoico. Montevideo, Uruguay: DIRAC, Fac. Ciencias 3:37–106
Matté V, Sommer CA, Lima EF, Philipp RP, Basei MAS (2016) Post-collisional ediacaran volcanism in oriental ramada plateau, southern Brazil. J S Am Earth Sci 71:201–222. https://doi.org/10.1016/j.jsames.2016.07.015
Menezes M, Schmitt RS, Ribeiro A, Nummer A, Cabrera J, Bossi J, Gaucher C (2010) Geologia Estructural e estratigrafia da Formacao Rocha, SE do Uruguai. In: VI Congreso Uruguayo de Geologia, Resumenes (CDROM)
Milani L, Kinnaird JA, Lehmann J, Naydenov KV, Saalmann K, Frei D, Gerdes A (2015) Role of crustal contribution in the early stage of the Damara Orogen, Namibia: new constraints from combined U–Pb and Lu–Hf isotopes from the Goas Magmatic Complex. Gondwana Res 28:961–986. https://doi.org/10.1016/j.gr.2014.08.007
Naidoo T, Zimmermann U, Vervoort J, Tait J (2017) The elusive snowball earth: U–Pb zircon ages from the upper diamictite of the Gifberg Group, South Africa. J Afr Earth Sci 129:307–317. https://doi.org/10.1016/j.jafrearsci.2017.01.015
Oriolo S, Oyhantçabal P, Wemmer K, Heidelbach F, Pfänder J, Basei MAS, Hueck M, Hannich F, Sperner B, Siegesmund S (2016) Shear zone evolution and timing of deformation in the Neoproterozoic transpressional Dom Feliciano Belt, Uruguay. J Struct Geol 92:59–78. https://doi.org/10.1016/j.jsg.2016.09.010
Oriolo S, Oyhantçabal P, Wemmer K, Siegesmund S (2017) Contemporaneous assembly of Western Gondwana and final Rodinia break-up: implications for the supercontinent cycle. Geosci Front 8(6):1431–1445. https://doi.org/10.1016/j.gsf.2017.01.009
Oriolo S, Schulz B, Gonzalez PD, Bechis F, Olaizola E, Krause J, Renda EM, Vizan H (2019) The late Paleozoic tectonometamorphic evolution of Patagonia revisited: insights from the pressure-temperature-deformation-time (P-T-D-t) path of the Gondwanide basement of the north Patagonian Cordillera (Argentina). Tectonics 38:2378–2400. https://doi.org/10.1029/2018TC005358
Oriolo S, Becker T (2018) The Kalahari Craton, Southern Africa: From Archean crustal evolution to Gondwana Amalgamation. In: Siegesmund S, Basei MAS, Oyhantçabal P, Oriolo S (eds) Geology of Southwest Gondwana. Regional Geology Reviews. Springer, Cham. https://doi.org/10.1007/978-3-319-68920-3_6
Oyhantçabal P, Siegesmund S, Wemmer K, Frei R, Layer P (2007) Post-collisional transition from calc alkaline to alkaline magmatism during transcurrent deformation in the southernmost Dom Feliciano Belt (Braziliano–Pan-African, Uruguay). Lithos 98(1–4):141–159. https://doi.org/10.1016/j.lithos.2007.03.001
Oyhantçabal P, Siegesmund S, Wemmer K, Presnyakov S, Layer P (2009) Geochronological constraints on the evolution of the southern Dom Feliciano Belt (Uruguay). J Geol Soc 166(6):1075–1084. https://doi.org/10.1144/0016-76492008-122
Oyhantçabal P, Siegesmund S, Wemmer K, Layer P (2010) The Sierra Ballena Shear Zone in the southernmost Dom Feliciano Belt (Uruguay): evolution, kinematics, and deformation conditions. Int J Earth Sci 99(6):1227–1246. https://doi.org/10.1007/s00531-009-0453-1
Oyhantçabal P, Eimer-Wagner M, Wemmer K, Schulz B, Frei R, Siegesmund S (2012) Paleo- and Neoproterozoic magmatic and

tectonometamorphic evolution of the Isla Cristalina de Rivera (Nico Pérez Terrane, Uruguay). Int J Earth Sci 101(7):1745–1762. https://doi.org/10.1007/s00531-012-0757-4

Oyhantçabal P, Oriolo S, Wemmer K, Basei MAS, Frei D, Siegesmund S (2020) Provenance of metasedimentary rocks of the western Dom Feliciano Belt in Uruguay: Insights from U–Pb detrital zircon geochronology, Hf and Nd model ages, and geochemicalal data. J S Am Earth Sci 108:103139. https://doi.org/10.1016/j.jsames.2020.103139

Oyhantcabal P, Siegesmund S, Wemmer K (2011) The Río de la Plata Craton: a review of units, boundaries, ages and isotopic signature. Int J Earth Sci 100:201–220. https://doi.org/10.1007/s00531-010-0580-8

Oyhantçabal P, Oriolo S, Philipp RP, Wemmer K, Siegesmund S (2018) The Nico Pérez Terrane of Uruguay and Southeastern Brazil. In: Siegesmund S, Basei MAS, Oyhantcabal P, Oriolo S (eds) Geology of Southwest Gondwana. Regional Geology Reviews. Springer, Cham. https://doi.org/10.1007/978-3-319-68920-3_7

Oyhantçabal P (2005) The Sierra Ballena Shear zone: kinematics, timing and its significance for the geotectonic evolution of southeast Uruguay. PhD thesis. University of Göttingen, Germany.

Passchier CW, Trouw RAJ, Ribeiro A, Paciullo FVP (2002) Tectonic evolution of the southern Kaoko Belt, Namibia. J Afr Earth Sci 35(1):61–75. https://doi.org/10.1016/S0899-5362(02)00030-1

Passchier CW, Trouw R, Schmitt RS (2016) How to make a transverse triple junction—new evidence for the assemblage of Gondwana along the Kaoko-Damara belts, Namibia. Geology 44(10):843–846. https://doi.org/10.1130/G38015.1

Patiño-Douce AE (1999) What do experiments tell us about the origin of granitic magmas? Geol Soc Spec Publ 168:55–75. https://doi.org/10.1144/GSL.SP.1999.168.01.05

Pearce J, Bender JF, De Long SE, Kidd WSF, Low PJ, GiJner Y, Saroglu F, Yilmaz Y, Moorbathg S, Mitchell JG (1990) Genesis of collision volcanism in Eastern Anatolia, Turkey. J Volcanol Geotherm Res 44(1–2):189–229. https://doi.org/10.1016/0377-0273(90)90018-B

Pecoits E, Konhauser KO, Aubet NR, Heaman LM, Veroslavsky G, Stern RA, Gingras MK (2012) Bilaterian burrows and grazing behavior at > 585 million years ago. Science 336(6089):1693–1696. https://doi.org/10.1126/science.1216295

Peel E, Sánchez Betucci L, Basei MAS (2018) Geology and geochronology of Paso del Dragón Complex (northeastern Uruguay): implications on the evolution of the Dom Feliciano Belt (Western Gondwana). J S Am Earth Sci 85:250–262. https://doi.org/10.1016/j.jsames.2018.05.009

Peel E (2012) Petrografia, geoquímica e geocronologia do Complexo Paso del Dragon, nordeste do Uruguai: implicaçaoes na evoluçao tectonica do Cinturao Dom Feliciano. PhD thesis. Universidade de Sao Paulo, Sao Paulo, p 198

Percival JJ, Konopásek J, Eiesland R, Sláma J, de Campos RS, Battisti MA, de Fátima BM (2021) Pre-orogenic connection of the foreland domains of the Kaoko-Dom Feliciano-Gariep orogenic system. Precambrian Res 354:106060. https://doi.org/10.1016/j.precamres.2020.106060

Petrolli L (2017) Caracterização estrutural, petrografia, geoquímica e geologia isotópica dos gnaisses Chácara das Pedras, NE do Cinturão Dom Feliciano, RS. MSc thesis. Porto Alegre: IGEO/UFRGS

Philipp RP, Machado R (2005) The Neoproterozoic to Cambrian granitic magmatism of Pelotas Batholith, Southern Brazil. J S Am Earth Sci 19(4):461–478. https://doi.org/10.1016/j.jsames.2005.06.010

Philipp RP, Bitencourt MF, Junges SL (2008) Isótopos de Nd dos Complexos Neoproterozóicos Cambaí e Cambaizinho, Terreno Vila Nova: implicações para a evolução do Cinturão Dom Feliciano no RS. Congresso Brasileiro de Geologia, vol 46. SBG, Anais, Curitiba, p 21

Philipp RP et al (2014) Oldest age of magmatism in the Passinho arc in the southwestern portion of Gondwana, Rio Grande do Sul, Brazil. In: 9 South American symposium on isotope Geology, Abstracts. São Paulo, p 186

Philipp RP, Pimentel MM, Chemale F Jr (2016) Tectonic evolution of the Dom Feliciano Belt in Southern Brazil: geological relationships and U–Pb geochronology. Braz J Geol 46(1):83–104. https://doi.org/10.1590/2317-4889201620150016

Philipp RP, Pimentel MM, Basei MAS (2018) The tectonic evolution of the Sao Gabriel Terrane, Dom Feliciano Belt, Southern Brazil: The Closure of the Charrua Ocean. In: Siegesmund S, Oyhantçabal P, Basei MAS, Oriolo S (eds) Geology of Southwest Gondwana. Regional Geology Reviews. Springer, Cham. https://doi.org/10.1007/978-3-319-68920-3_10

Philipp RP, Pimentel MM, Basei MAS, Salvi M, De Lena LOF, Vedana LA, Gubert ML, Lopes CG, Laux JH, Camozzato E (2021) U–Pb detrital zircon dating applied to metavolcano-sedimentary complexes of the São Gabriel Terrane: new constraints on the evolution of the Dom Feliciano Belt. J S Am Earth Sci 110:103409. https://doi.org/10.1016/j.jsames.2021.103409

Preciozzi F, Masquelin H, Basei MAS (1999) The Namaqua/Grenville Terrane of eastern Uruguay. In: II South American Symposium on Isotope Geology. Córdoba, Argentina, pp 338–340

Preciozzi F, Sanchez Bettucci L, Basei MAS (2002) Punta del Este terrane: a better knowledge; El terreno Punta del este: una aproximacion al conocimiento. II. Colloquio Internacional Vendiano-Cambrico del Gondwana Occidental, 7.-8.03.2002, Montevideo Uruguay. ISBN: 9974-0-0178-1, pp 1–28

Preciozzi F, Basei M, Peel E (2003) Punta del Este Terrane: Mesoproterozoic and Neoproterozoic cover. IV South American Symposium on Isotope Geology. Salvador Brazil. ISSN 1679-3684, pp 660–661

Preciozzi F (1993) Petrography and geochemistry of five granitic plutons from south-central Uruguay. Contribution to the knowledge of the Piedra Alta Terrane. Unpublished PhD thesis, Université du Québec, p 143

Qin JF, Lai SC, Long XP, Li YF, Ju YJ, Zhao SW, Zhu RZ, Wang JB, Zhang ZZ (2018) Hydrous melting of metasomatized mantle wedge and crustal growth in the post-collisional stage: evidence from Late Triassic monzodiorite and its mafic enclaves in the south Qinling (central China). Lithosphere 11(1):3–20. https://doi.org/10.1130/L1006.1

Ramos RC, Koester E (2015) Lithogeochemistry of the meta-igneous units from Arroio Grande Ophiolitic Complex, southernmost Brazil. Braz J Geol 45(1):65–78. https://doi.org/10.1590/23174889201500010005

Ramos RC, Koester E, Vieira DT, Porcher CC, Gezatt JN, Silveira RL (2018) Insights on the evolution of the Arroio Grande ophiolite (Dom Feliciano belt, Brazil) from Rb–Sr and SHRIMP U–Pb isotopic geochemistry. J S Am Earth Sci 86:38–53. https://doi.org/10.1016/j.jsames.2018.06.004

Ramos RC, Koester E, Vieira DT (2019) Plagioclase-hornblende geothermo-barometry of metamafites from the Arroio Grande Ophiolite, Dom Feliciano Belt, southernmost Brazil. J S Am Earth Sci. https://doi.org/10.1016/j.jsames.2018.06.004

Ramos RC, Koester E, Vieira DT (2020) Sm–Nd systematics of metaultramafic-mafic rocks from the Arroio Grande Ophiolite (Brazil): Insights on the evolution of the South Adamastor paleo-ocean. Geosci Front 11(6):2287–2296. https://doi.org/10.1016/j.gsf.2020.02.013

Ramos RC, Koester E, Porcher CC (2017) Chemistry of chromites from Arroio Grande Ophiolite (Dom Feliciano Belt, Brazil) and their possible connection with the Nama Group (Namibia). J

S Am Earth Sci 80:192–206. https://doi.org/10.1016/j.jsames.2017.09.032

Rapela C, Fanning CM, Casquet C, Pankhurst RJ, Spalletti L, Poiré D, Baldo EG (2011) The Rio de la Plata craton and the adjoining Pan-African/brasiliano terranes: their origins and incorporation into south-west Gondwana. Gondwana Res 20(4):673–690. https://doi.org/10.1016/j.gr.2011.05.001

Remus MVD (1991) Geologia e Geoquímica do Complexo Cambaizinho, São Gabriel—RS. MSc thesis, Universidade Federal do Rio Grande do Sul, UFRGS, Brasil

Rino S, Kon Y, Sato W, Maruyama S, Santosh M, Zhao D (2008) The Grenvillian and Pan-African orogens: World's largest orogenies through geologic time, and their implications on the origin of superplume. Gondwana Res 14(1–2):51–72. https://doi.org/10.1016/j.gr.2008.01.001

Saalmann K, Gerdes A, Lahaye Y, Hartmann LA, Remus MVD, Läufer A (2011) Multiple accretion at the eastern margin of the Rio de la Plata craton: the prolonged Brasiliano orogeny in southernmost Brazil. Int J Earth Sci 100(2):355–378. https://doi.org/10.1007/s00531-010-0564-8

Santos JOS, Hartmann LA, Bossi J, Campal N, Schipilov A, Piñeyro D, McNaughton NJ (2003) Duration of the Trans-Amazonian cycle and its correlation within South America based on U–Pb SHRIMP geochronology of the La Plata Craton, Uruguay. Int Geol Rev 45(1):27–48. https://doi.org/10.2747/0020-6814.45.1.27

Sawyer EW, Cesare B, Brown M (2011) When the continental crust melts. Elements 7(4):229–234. https://doi.org/10.2113/gselements.7.4.229

Seth B, Kröner A, Mezger K, Nemchin AA, Pidgoen RT, Okrusch M (1998) Archaean to Neoproterozoic magmatic events in the Kaoko Belt of NW Namibia and their geodynamic significance. Precambr Res 92(4):341–363. https://doi.org/10.1016/S0301-9268(98)00086-2

Siegesmund S, Basei MA, Oyhantçabal P, Oriolo S (eds) (2018) Geology of Southwest Gondwana. Springer

Silva Filho BC, Soliani E Jr (1987) Origem e evolução dos Gnaisses Cambaí: exemplo de estudo integrado de análise estrutural, petroquímica e geocronologia. Atas, II. Simpósio Sul Brasileiro De Geologia 1:127–146

Silva Lara H, Siegesmund S, Wemmer K, Hueck M, Basei MAS, Oyhantçabal P (2021) The Sierra de Aguirre Formation, Uruguay: post-collisional Ediacaran volcanism in the southernmost Dom Feliciano Belt. J S Am Earth Sci 107:103118. https://doi.org/10.1016/j.jsames.2021.103118

Söderlund U, Patchett PJ, Vervoort JD, Isachsen CE (2004) The 176Lu decay constant determined by Lu-Hf and U-Pb isotope systematics of Precambrian mafic intrusions. Earth Planet Sci Lett 219:311–324

Soliani E Jr (1986) Os dados geocronológicos do Escudo Sul-riograndense e suas implicações de ordem geotectônica. PhD thesis, Universidade São Paulo, p 425

Sommer CA, Lima EF, Pierosan R, Machado A (2011) Reoignimbritos e ignimbritos de alto grau do Vulcanismo Acampamento Velho, RS: origem e temperatura de formação. Rev Bras Geociênc 41(3):420–435

Sommer CA, Leitzke FP, de Lima EF, Barreto CJS, Lafon JM, Matté V, Philipp RP, Conceicao RV, Basei MAS (2017) Zircon U–Pb geochronology, Sm–Nd and Pb–Pb isotope systematics of Ediacaran post-collisional high-silica Acampamento Velho volcanism at the Tupanci area, NW of the Sul-Rio-Grandense Shield, Brazil. Braz J Geol 47(4):545–560. https://doi.org/10.1590/2317-4889201720170064

Spoturno JJ, Oyhantçabal P, Loureiro J (2012) Mapa geológico del Departamento de Maldonado escala 1:100.000. Facultad de Ciencias (UdelaR)—Dirección Nacional de Minería y Geología (MIEM), Montevideo, Uruguay

Studies of the Nico Perez Terrane, Reworked Río de la Plata Craton, Uruguay. Short Papers. IV South American Symposium on Isotope Geology, Salvador, Brazil

Tambara GB, Koester E, Ramos RC, Porcher CC, Vieira DT, Fernandes LA, Lenz C (2019) Geoquímica e geocronologia dos Gnaisses Piratini: magmatismo cálcio-alcalino médio a alto-K de 784 Ma (U–Pb SHRIMP) no SE do Cinturão Dom Feliciano (RS, Brasil). Pesqui em Geociênc 46(2):e0769. https://doi.org/10.22456/1807-9806.95466

Teixeira W (1982) Folhas SH.22—Porto Alegre, SI.22—Lagoa Mirim e SH.21—Uruguaiana. Interpretação dos Dados Radiométricos e Evolução Geocronológica. Projeto RADAM BRASIL, Florianópolis (Relatório Interno, Inédito)

Turner S, Arnaud N, Liu J, Rogers N, Hawkesworth C, Harris N, Kelley S, Van Calsteren P, Deng W (1996) Post-collision, Shoshonitic Volcanism on the Tibetan Plateau: implications for Convective Thinning of the Lithosphere and the Source of Ocean Island Basalts. J Petrol 37(1):45–71. https://doi.org/10.1093/petrology/37.1.45

Van Schijndel V, Cornell DH, Frei D, Simonsen SL, Whitehouse MJ (2014) Crustal evolution of the Rehoboth Province from Archaean to Mesoproterozoic times: insights from the Rehoboth Basement Inlier. Precambrian Res 240:22–36. https://doi.org/10.1016/j.precamres.2013.10.014

Vermeesch P (2012) On the visualisation of detrital age distributions. Chem Geol 312313:190–194. https://doi.org/10.1016/j.chemgeo.2012.04.021

Vieira DT, Porcher CC, Koester E, Ramos RC, da Silva M, Gross AO, Masquelin H, Fernandes LAD (2019) Chafalote Metamorphic Suite (Uruguay): reflections on the evolution of the Punta del Este Terrane. J S Am Earth Sci 98:102420. https://doi.org/10.1016/j.jsames.2019.102420

Vieira DT, Koester E, Porcher CC (2016) Magmatismo Neoproterozóico (680 Ma) no sudeste do escudo Sul-Rio-Grandense: U–Pb e Lu–Hf LA–MC–ICP–MS em zircão. 48th Congresso Brasileiro de Geologia, Porto Alegre, Brazil. http://sbg.sitepessoal.com/anais48cbg/sts/st13.htm (ID 8889)

Will TM, Frimmel HE, Gaucher C, Bossi J (2014) Geochemical and isotopic composition of Pan-African metabasalts from southwestern Gondwana: evidence of Cretaceous South Atlantic opening along a Neoproterozoic back-arc. Lithos 202:363–381. https://doi.org/10.1016/j.lithos.2014.05.034

Will TM, Gaucher C, Ling XX, Li XH, Li QL, Frimmel HE (2019) Neoproterozoic magmatic and metamorphic events in the Cuchilla Dionisio Terrane, Uruguay, and possible correlations across the South Atlantic. Precambrian Res. https://doi.org/10.1016/j.precamres.2018.11.004

Will TM, Höhn S, Frimmel HE, Gaucher C, Le Roux PJ, Macey PH (2020) Petrological, geochemical and isotopic data of Neoproterozoic rock units from Uruguay and South Africa: correlation of basement terranes across the South Atlantic. Gondwana Res 80:12–32. https://doi.org/10.1016/j.gr.2019.10.012

Will TM, Gaucher C, Ling XX, le Roux JP, Li XH, Li QL (2021) Ediacaran bimodal volcanism in the southernmost Dom Feliciano Belt, Uruguay: implications for the evolution of SW Gondwana. Lithos 406–407:106539. https://doi.org/10.1016/j.lithos.2021.106539

Yang JH, Wu FY, Wilde SA, Xie LW, Yang YH, Liu XM (2007) Tracing magma mixing in granite genesis: in-situ U–Pb dating and Hf isotope analysis of zircons. Contrib Mineral Petrol 153(2):177–190. https://doi.org/10.1007/s00410-006-0139-7

Zeh A, Gerdes A (2012) U–Pb and Hf isotope record of detrital zircons from gold-bearing sediments of the Pietersburg Greenstone Belt (South Africa)—Is there a common provenance with the

Witwatersrand Basin? Precambrian Res 204–205:46–56. https://doi.org/10.1016/j.precamres.2012.02.013

Zeh A, Gerdes A, Klemd R, Barton JM Jr (2007) Archaean to Proterozoic crustal evolution in the Central Zone of the Limpopo Belt (South Africa-Botswana): constraints from combined U–Pb and Lu–Hf isotope analyses of zircon. J Petrol 48(8):1605–1639. https://doi.org/10.1093/petrology/egm032

Zeh A, Gerdes A, Klemd R, Barton JM Jr (2008) U–Pb and Lu–Hf isotope record of detrital zircon grains from the Limpopo Belt-Evidence for crustal recycling at the Hadean to early-Archean transition. Geochim Cosmochim Acta 72(21):5304–5329. https://doi.org/10.1016/j.gca.2008.07.033

Zeh A, Gerdes A, Barton JM Jr, Klemd R (2010) U–Th–Pb and Lu–Hf systematics of zircon from TTG's, leucosomes, anorthosites and quartzites of the Limpopo Belt (South Africa): constraints for the formation, recycling, and metamorphism of Paleoarchean crust. Precambrian Res 179(1–4):50–68. https://doi.org/10.1016/j.precamres.2010.02.012

Zeh A, Gerdes A, Heubeck C (2013a) U–Pb and Hf isotope data of detrital zircons from the Barberton Greenstone Belt: constraints on provenance and Archaean crustal evolution. J Geol Soc Lond 170:215–223. https://doi.org/10.1144/jgs2011-162

Zeh A, Jaguin J, Poujol M, Boulvais P, Block S, Paquette JL (2013b) Juvenile crust formation in the northeastern Kaapvaal Craton at 2.97 Ga—implications for Archean terrane accretion, and the source of the Pietersburg gold. Precambrian Res 233:20–43. https://doi.org/10.1016/j.precamres.2013.04.013

Zeh A, Stern R, Gerdes A (2014) The oldest zircons of Africa—their U–Pb–Hf–O isotope and trace element systematics, and implications for Hadean to Archean crust-mantle evolution. Precambrian Res 241:203–230. https://doi.org/10.1016/j.precamres.2013.11.006

Zeh A, Gerdes A, Barton JM Jr (2009) Archean accretion and crustal evolution of the Kalahari Craton—the Zircon age and Hf isotope record of granitic rocks from Barberton/Swaziland to the Francistown Arc. J Petrol 5085:933–966. https://doi.org/10.1093/petrology/egp027

Zeh A, Gerdes A, Millonig L (2011) Hafnium isotope record of the Ancient GneissComplex, Swaziland, southern Africa: evidence for Archaean crust-mantle formation and crust reworking between 3.66 and 2.73 Ga. J Geol Soc Lond 168(4):953–963. https://doi.org/10.1144/0016-76492010-117

Zirakparvar NA, Mathez EA, Scoates JS, Wall CJ (2014) Zircon Hf isotope evidence for an enriched mantle source for the Bushveld Igneous complex. Contrib Mineral Petrol 168:1050. https://doi.org/10.1007/s00410-014-1050-2